ULB-TH/14-03

Scalar triplet flavored leptogenesis: a systematic approach

D. Aristizabal Sierra[a,1], Mikaël Dhen[b,2], Thomas Hambye[b,3]

[a]*IFPA, Dep. AGO, Université de Liège, Bat B5, Sart Tilman B-4000 Liege 1, Belgium.*

[b]*Service de Physique Théorique, Université Libre de Bruxelles Bld du Triomphe, CP225, 1050 Brussels Belgium.*

Abstract

Type-II seesaw is a simple scenario in which Majorana neutrino masses are generated by the exchange of a heavy scalar electroweak triplet. When endowed with additional heavy fields, such as right-handed neutrinos or extra triplets, it also provides a compelling framework for baryogenesis via leptogenesis. We derive in this context the full network of Boltzmann equations for studying leptogenesis in the flavored regime. To this end we determine the relations which hold among the chemical potentials of the various particle species in the thermal bath. This takes into account the standard model Yukawa interactions of both leptons and quarks as well as sphaleron processes which, depending on the temperature, may be classified as faster or slower than the Universe Hubble expansion. We find that when leptogenesis is enabled by the presence of an extra triplet, lepton flavor effects allow the production of the $B-L$ asymmetry through lepton number conserving CP asymmetries. This scenario becomes dominant as soon as the triplets couple more to leptons than to standard model scalar doublets. In this case, the way the $B-L$ asymmetry is created through flavor effects is novel: instead of invoking the effect of L-violating inverse decays faster than the Hubble rate, it involves the effect of L-violating decays slower than the Hubble rate. We also analyze the more general situation where lepton number violating CP asymmetries are present and actively participate in the generation of the $B-L$ asymmetry, pointing out that as long as L-violating triplet decays are still in thermal equilibrium when the triplet gauge scattering processes decouple, flavor effects can be striking, allowing to avoid all washout suppression effects from seesaw interactions. In this case the amount of $B-L$ asymmetry produced is limited only by a universal gauge suppression effect, which nevertheless goes away for large triplet decay rates.

[1]e-mail addresses: daristizabal@ulg.ac.be
[2]e-mail address: mikadhen@ulb.ac.be
[3]e-mail address: thambye@ulb.ac.be

1 Introduction

Non-vanishing neutrino masses [1, 2, 3], and the cosmic asymmetry between baryons and anti-baryons [4, 5], constitute two well-established experimental facts which have particularly well demonstrated that physical degrees of freedom beyond the standard model (SM) must be at work at certain unknown energy scale. Although a large number of scenarios capable of accounting for these experimental facts exist, arguably the tree-level seesaw models, type-I [6], type-II [7] and type-III [8], are of special interest: they constitute the simplest frameworks, are well theoretically motivated and, through the leptogenesis mechanism, provide a common explanation for both puzzles (for reviews see [9, 10] and [11]).

The type-II leptogenesis scenario [11, 12, 13, 14, 15], in which the baryon asymmetry is generated from the decay of one or several scalar triplets, is more intricate than the standard scenario based in the type-I seesaw. First of all, while leptogenesis in type-I seesaw is driven by right-handed (RH) neutrinos which do not couple to gauge bosons, in type-II seesaw (as well as in type-III seesaw) the states which dynamically generate the $B-L$ asymmetry do have electroweak interactions. Since at high temperatures gauge reactions are much more faster than the Universe Hubble expansion, one may be tempted to believe that gauge couplings constitute a non-circumventable obstacle which unavoidably imply the inviability of leptogenesis in these scenarios. This however is not the case [11, 13, 15, 16, 17, 18]. Once the temperature of the heat bath reaches the mass of the decaying triplet, gauge reactions—being doubly Boltzmann suppressed—rapidly decouple and the dynamics becomes dominated by Yukawa reactions which then operate to a large extent as in the type-I seesaw case. Secondly, while a single scalar triplet suffices for fitting neutrino masses and mixing angles, leptogenesis requires extra degrees of freedom (e.g. in the form of extra heavier triplets or RH neutrinos). Thirdly, since the scalar triplet is not a self-conjugated particle as a RH neutrino is, a scalar triplet/anti-triplet asymmetry develops [15, 11], thus calling for an additional Boltzmann equation accounting for the new asymmetry populating the heat bath. As a result, while the SM scalar asymmetry in the type-I case is fully determined by the evolution of the $B-L$ asymmetry, here it is determined in addition by the evolution of the triplet scalar asymmetry.

Certainly one of the main differences between type-I and type-II seesaws resides on the feasibility of on-shell collider production of the seesaw states. At LHC scalar triplet production proceeds mainly via gauge boson exchange, with a cross-section which depending on the triplet mass can be as large as $\sim 1\,\mathrm{pb}^{-1}$ [19, 20]. Subsequent decay of the scalar triplet, in particular to the dilepton channel, combined with possible displaced vertices may eventually allow the reconstruction of the Lagrangian parameters, as has been shown in [19]. Production, however, requires the scalar triplet to be below $\sim 1\,\mathrm{TeV}$, mass values for which producing a baryon asymmetry consistent with data is not possible due to late $B-L$ production and electroweak sphaleron decoupling [15, 21], a result which even in the flavored regime remains valid (see a similar discussion for leptogenesis in the type-III seesaw framework in [17]).

In this paper we aim to study the generation of the $B-L$ asymmetry arising from the CP violating and out-of-equilibrium decays of a scalar triplet, taking into account in a systematic way any relevant effect that a SM interaction could have at a given temperature. This includes the flavor effects of the charged lepton Yukawa couplings[1] and the "spectator" effects of the quark Yukawa couplings (in particular the role of the top Yukawa reaction) and the sphalerons processes. To this end, we will first derive the full network of flavored Boltzmann equations and then will consider the redistribution of the $B/3-L_i$ asymmetries in the heat bath, which in turn requires considering the conservation laws and chemical equilibrium conditions implied by slow and fast reactions.

With these tools at hand, and in order to illustrate how does scalar triplet flavored leptogenesis works, we will analyze two scenarios. (i) A scenario where the extra degrees of freedom correspond to additional scalar triplets, with the lepton number conserving CP flavored asymmetries naturally dominating the generation of the $B-L$ asymmetry (purely flavored leptogenesis (PFL) scenario [24, 25, 26, 27]); (ii) general triplet leptogenesis models involving lepton number violating CP asymmetries stemming from the presence of any seesaw state heavier than the decaying scalar triplet (RHNs, fermion or extra scalar electroweak triplets).

The paper is organized as follows. In Sec. 2 we fix our notation, discuss tree-level triplet decays, neutrino mass generation and the different CP asymmetries. In Sec. 3 we derive the network of flavored and unflavored Boltzmann equations, discuss chemical equilibration and analytical solutions to the flavored Boltzmann equations. In Secs. 4 and 5 we study scenarios (i) and (ii). Finally in Sec. 6 we present our conclusions. In Appx. A we present useful formulæ.

2 Generalities

As regards the CP asymmetries, the details of scalar triplet leptogenesis strongly depend on the extra beyond SM degrees of freedom. As already pointed out, here we aim to analyze two generic scenarios: (i) models featuring several scalar triplets, or in other words extended pure type-II seesaw models, focusing on the cases where the $B-L$ asymmetry production is dominated by the lepton conserving CP asymmetries; (ii) models involving a scalar triplet (minimal type-II seesaw) and heavier seesaw states, more specifically focusing on the effects of the lepton number violating asymmetries. The latter are particularly relevant for models where the generation of a $B-L$ asymmetry becomes possible due to the interplay between type-I and type-II seesaws, scenarios arising in many well-motivated gauge extensions of the SM.

[1] The role played by lepton flavor effects in production as well as the evolution of the flavored $B/3-L_i$ asymmetries have been partially considered in Ref. [23].

2.1 Interactions and tree-level triplet decays

The new interactions induced by extending both the scalar and fermion sectors of the SM with n_Δ scalar $SU(2)$ triplets (Δ_α) and n_R RH neutrinos (N_α) can be written, in the basis in which the RH neutrino Majorana and charged lepton mass matrices are diagonal, according to

$$\mathcal{L}^{(I)} = i\overline{N_\alpha}\not{\partial}N_\alpha - \overline{N_\alpha}\lambda_{\alpha i}\tilde{\phi}^\dagger \ell_{L_i} - \frac{1}{2}\overline{N_\alpha}M_{N_{\alpha\alpha}}C\bar{N}_\alpha^T + \text{H.c.} \tag{1}$$

$$\begin{aligned}\mathcal{L}^{(II)} = &\left(D_\mu \vec{\Delta}_\alpha\right)^\dagger \left(D^\mu \vec{\Delta}_\alpha\right) - \vec{\Delta}_\alpha^\dagger m^2_{\Delta_\alpha}\vec{\Delta}_\alpha \\ &+ \ell_{L_i}^T C\, i\tau_2\, Y_\alpha^{ij}\left(\frac{\vec{\tau}\cdot\vec{\Delta}_\alpha}{\sqrt{2}}\right)\ell_{L_j} + \mu_{\Delta_\alpha}\tilde{\phi}^\dagger\left(\frac{\vec{\tau}\cdot\vec{\Delta}_\alpha}{\sqrt{2}}\right)^\dagger \phi + \text{H.c.}\,,\end{aligned} \tag{2}$$

with $\ell_L^T = (\nu_L, e_L)$ and $\phi^T = (\phi^+, (v + h^0 + i\phi_3^0)/\sqrt{2})$ the leptons and scalar boson $SU(2)$ doublets, $\tilde{\phi} = i\tau_2\phi^*$, $\vec{\tau}^T = (\tau_1, \tau_2, \tau_3)$ (with τ_i the 2×2 Pauli matrices) and the scalar Δ_α triplets given in the $SU(2)$ fundamental representation i.e. $\Delta_\alpha = (\Delta_\alpha^1, \Delta_\alpha^2, \Delta_\alpha^3)$. Here Y_α and λ are 3×3 and $n_R \times 3$ Yukawa matrices in flavor space and C is the charge conjugation matrix. Throughout the text we will be denoting lepton flavors e, μ, τ with Latin indices $i, j, k\ldots$ while RH neutrinos and scalar triplets with Greek labels $\alpha, \beta, \ldots$. The covariant derivative in (2) reads

$$D_\mu = \partial_\mu - ig\vec{T}\cdot\vec{W}_\mu - ig' B_\mu\,, \tag{3}$$

where $\vec{T}$ are the dimension three representations of the $SU(2)$ generators. In our notation the $SU(2)$ components of the fundamental scalar triplet representation have not all well defined electric charges, electric charge eigenstates are instead given by

$$\boldsymbol{\Delta_\alpha} \equiv \frac{\vec{\tau}\cdot\vec{\Delta}_\alpha}{\sqrt{2}} = \begin{pmatrix} \frac{\Delta_\alpha^+}{\sqrt{2}} & \Delta_\alpha^{++} \\ \Delta_\alpha^0 & -\frac{\Delta_\alpha^+}{\sqrt{2}}\end{pmatrix}\,, \tag{4}$$

with the different components reading as

$$\Delta_\alpha^0 = \frac{1}{\sqrt{2}}\left(\Delta_\alpha^1 + i\Delta_\alpha^2\right)\,, \qquad \Delta_\alpha^+ = \Delta_\alpha^3\,, \qquad \Delta_\alpha^{++} \equiv \frac{1}{\sqrt{2}}\left(\Delta_\alpha^1 - i\Delta_\alpha^2\right)\,. \tag{5}$$

In a general setup as the one determined by Eqs. (1) and (2) the number of independent parameters, determined by the Yukawa coupling and mass matrices, is given by $4n_R$ moduli and $3(n_R-1)$ CP phases in the type-I sector, while by $8n_\Delta$ moduli and $3(2n_\Delta-1)$ CP phases in the type-II sector.

The scalar interactions in (2) induce non-vanishing triplet vacuum expectation values which can be calculated from the minimization of the scalar potential: $\langle\Delta_\alpha\rangle = v_{\Delta_\alpha} \simeq \mu_{\Delta_\alpha} v^2/2m^2_{\Delta_\alpha}$.

Both Lagrangians in (1) and (2), involving lepton number violating sources (from the coexistence of λ and M_N and of Y and μ_Δ), induce tree-level light neutrino Majorana

masses through the standard type-I (assuming $v\,\lambda\cdot M_N^{-1}\ll 1$) and type-II seesaw mechanisms. The structure of the full neutrino mass matrix will of course depend on whether a single or both mechanisms intervene. Since here we will be dealing with scenarios determined by either the setup of Eq. (2) or an interplay between (1) and (2), in what follows we write the effective neutrino mass matrix in each case, namely

$$\mathcal{M}_\nu^{(II)} = \sum_\alpha \mathcal{M}_{\Delta_\alpha}^\nu = \sum_\alpha \mu_{\Delta_\alpha}\frac{v^2}{m_{\Delta_\alpha}^2}Y_\alpha \ , \tag{6}$$

$$\mathcal{M}_\nu^{(I+II)} = \sum_\alpha \mathcal{M}_{\Delta_\alpha}^\nu + \mathcal{M}_N^\nu = \sum_\alpha \mu_{\Delta_\alpha}\frac{v^2}{m_{\Delta_\alpha}^2}Y_\alpha - \frac{v^2}{2}\lambda^T M_N^{-1}\lambda \ . \tag{7}$$

The light neutrino mass spectrum is thus derived from these matrices by diagonalization through the leptonic mixing matrix $U = U(\theta_{23})U(\theta_{13},\delta)U(\theta_{12})\hat{P}$, with θ_{ij} being the neutrino mixing angles, δ the Dirac CP phase and $\hat{P} = \mathrm{diag}(1, e^{-i\varphi_1}, e^{-i\varphi_2})$ containing the Majorana CP phases.

Regardless of the scenario considered, we are interested in the $B-L$ asymmetry generated in triplet decays. Generating a sufficiently large $B-L$ asymmetry, that after sphaleron reconversion matches the observed baryon asymmetry, requires certain balance between production and washout. Production is controlled by the CP violating asymmetry (ϵ_{Δ_α}) which structure is determined by the details (interactions) of the corresponding scenario, but which in any case arises via the interference of the tree-level decay and its one-loop corrections, as required by the unitarity of the scattering matrix [28].

Tree-level triplet decays involve leptonic and scalar final states. The leptonic partial decay widths, depending on the lepton flavor composition of the final states, involve extra factors of 1/2 which avoid overcounting:

$$\Gamma(\Delta_\alpha \to \bar{\ell}_i\bar{\ell}_j) = \frac{m_{\Delta_\alpha}}{8\pi}|Y_\alpha^{ij}|^2\left[1+|Q-1|(1-\delta_{ij})\right] \ , \tag{8}$$

where Q stands for the electric charges of the different $SU(2)$ triplet components, $\Delta_\alpha^Q = (\Delta_\alpha^0, \Delta_\alpha^+, \Delta_\alpha^{++})$. On the other hand, scalar triplet decay modes can be written according to

$$\Gamma(\Delta_\alpha \to \phi\phi) = \frac{|\mu_{\Delta_\alpha}|^2}{8\pi m_{\Delta_\alpha}} \ , \tag{9}$$

so the total decay width, after summing over lepton flavors, can be written as

$$\Gamma_{\Delta_\alpha}^{\mathrm{Tot}} = \frac{1}{8\pi}\frac{m_{\Delta_\alpha}^2\tilde{m}_{\Delta_\alpha}}{v^2}\frac{B_\ell^\alpha + B_\phi^\alpha}{\sqrt{B_\ell^\alpha B_\phi^\alpha}} \ , \tag{10}$$

where the "neutrino mass-like" parameter $\tilde{m}_{\Delta_\alpha}$ is defined as

$$\tilde{m}_{\Delta_\alpha}^2 = |\mu_{\Delta_\alpha}|^2\frac{v^4}{m_{\Delta_\alpha}^4}\ \mathrm{Tr}[Y_\alpha Y_\alpha^\dagger] \ , \tag{11}$$

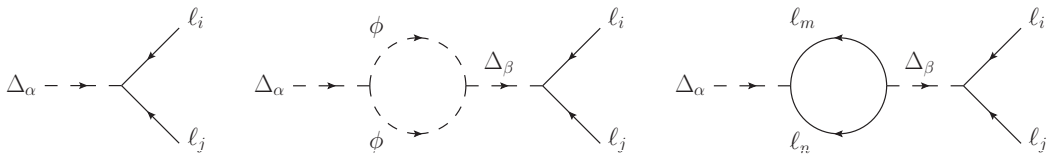

Figure 1: *Tree-level and one-loop Feynman diagrams responsible for the flavored CP asymmetry* $\epsilon^{\ell_i}_{\Delta_\alpha}$ *in the pure type-II seesaw scenario.*

with B^α_ℓ and B^α_ϕ standing for the Δ_α triplet decay branching ratios to lepton and scalar final states:

$$B^\alpha_\ell = \sum_{i=e,\mu,\tau} B^\alpha_{\ell_i} = \sum_{i,j=e,\mu,\tau} B_{\ell_{ij}} = \sum_{i,j=e,\mu,\tau} \frac{m_{\Delta_\alpha}}{8\pi\Gamma^{\rm Tot}_{\Delta_\alpha}} |Y^{ij}_\alpha|^2 \ ,$$
$$B^\alpha_\phi = \frac{|\mu_{\Delta_\alpha}|^2}{8\pi m_{\Delta_\alpha}\Gamma^{\rm Tot}_{\Delta_\alpha}} \ , \tag{12}$$

where of course the relation $B^\alpha_\ell + B^\alpha_\phi = 1$ holds. As can be seen directly from Eqs. (10) and (11), for fixed $\tilde{m}_{\Delta_\alpha}$ and m_{Δ_α}, $\Gamma^{\rm Tot}_{\Delta_\alpha}$ exhibits a minimum at $B^\alpha_\ell = B^\alpha_\phi = 1/2$. Thus, the farther we are from $B^\alpha_\ell = B^\alpha_\phi = 1/2$, the faster the scalar triplet decays.

2.2 CP asymmetries in triplet decays

As already pointed out, the one-loop corrections to the tree-level decay depend on the details of the corresponding model. In purely triplet models, that is to say models entirely determined by the Lagrangian in (2), the corrections to the leptonic tree-level decay mode involve only wave-function type corrections [12]. The CP asymmetry follows from the interference between the tree-level and wave-function corrections shown in Fig. 1, it therefore consists of two pieces: a lepton number and flavor violating one (scalar loops) and a purely flavor violating part (lepton loops). The total flavored CP asymmetry in Δ_α decays can then be written as

$$\epsilon^{\ell_i}_{\Delta_\alpha} = \epsilon^{\ell_i(\not{L},\not{F})}_{\Delta_\alpha} + \epsilon^{\ell_i(\not{F})}_{\Delta_\alpha} \ , \tag{13}$$

where the two pieces read

$$\epsilon^{\ell_i(\not{L},\not{F})}_{\Delta_\alpha} = \frac{1}{2\pi} \sum_{\beta\neq\alpha} \frac{\mathbb{I}{\rm m}\left[\left(Y^\dagger_\alpha Y_\beta\right)_{ii} \mu^*_{\Delta_\alpha}\mu_{\Delta_\beta}\right]}{m^2_{\Delta_\alpha}{\rm Tr}[Y_\alpha Y^\dagger_\alpha] + |\mu_{\Delta_\alpha}|^2} \, g(m^2_{\Delta_\alpha}/m^2_{\Delta_\beta}) \ , \tag{14}$$

$$\epsilon^{\ell_i(\not{F})}_{\Delta_\alpha} = \frac{1}{2\pi} \sum_{\beta\neq\alpha} m^2_{\Delta_\alpha} \frac{\mathbb{I}{\rm m}\left[\left(Y^\dagger_\alpha Y_\beta\right)_{ii} {\rm Tr}[Y_\alpha Y^\dagger_\beta]\right]}{m^2_{\Delta_\alpha}{\rm Tr}[Y_\alpha Y^\dagger_\alpha] + |\mu_{\Delta_\alpha}|^2} \, g(m^2_{\Delta_\alpha}/m^2_{\Delta_\beta}) \ , \tag{15}$$

with

$$g(x) = \frac{x(1-x)}{(1-x)^2 + xy} \tag{16}$$

and $y = (\Gamma^{\rm Tot}_{\Delta_\beta}/m_{\Delta_\beta})^2$. Branco:2011zb Note that the CP asymmetry in Eq. (14) is in-line with what has been found in [22], and that the one in Eq. (15) is in-line with what has been found in [23]. This piece, which we refer to as purely flavored CP violating asymmetry, satisfies the total lepton number conservation constraint

$$\sum_i \epsilon^{\ell_i(\not{L})}_{\Delta_\alpha} = 0 \ , \tag{17}$$

and so the total CP asymmetry can consequently be written as

$$\epsilon_{\Delta_\alpha} = \sum_{i=e,\mu,\tau} \epsilon^{\ell_i}_{\Delta_\alpha} = \sum_{i=e,\mu,\tau} \epsilon^{\ell_i(\not{L},\not{F})}_{\Delta_\alpha} \ . \tag{18}$$

In terms of triplet decay observables the total flavored asymmetries can be recasted according to

$$\epsilon^{\ell_i}_{\Delta_\alpha} = -\frac{1}{2\pi v^2}\sum_{\beta\neq\alpha}\frac{m^2_{\Delta_\beta}}{m_{\Delta_\alpha}}\frac{\sqrt{B^\alpha_\ell B^\alpha_\phi}}{\tilde{m}_{\Delta_\alpha}}\mathbb{I}{\rm m}\left[\left(\mathcal{M}^{\nu\dagger}_{\Delta_\alpha}\mathcal{M}^{\nu}_{\Delta_\beta}\right)_{ii}\left(1+\frac{m_{\Delta_\alpha}}{m_{\Delta_\beta}}\frac{{\rm Tr}[\mathcal{M}^{\nu}_{\Delta_\alpha}\mathcal{M}^{\nu\dagger}_{\Delta_\beta}]}{\tilde{m}_{\Delta_\alpha}\tilde{m}_{\Delta_\beta}}\sqrt{\frac{B^\alpha_\ell B^\beta_\ell}{B^\alpha_\phi B^\beta_\phi}}\right)\right] \times g(m^2_{\Delta_\alpha}/m^2_{\Delta_\beta}) \ . \tag{19}$$

If flavor effects are operative, that is to say if leptogenesis takes place below 10^{12} GeV, the purely flavored CP asymmetry in (15) will play a role in the generation of the $B-L$ asymmetry. These asymmetries, conserving total lepton number, involve only the Y_α Yukawa couplings and not the lepton number violating parameter μ_{Δ_α}. Hence, as also noted in Ref. [23], they are not necessarily suppressed by the smallness of the neutrino masses. As can be seen by comparing (14) and (15), when the condition

$$\mu^*_{\Delta_\alpha}\mu_{\Delta_\beta} \ll m^2_{\Delta_\alpha}{\rm Tr}[Y_\alpha Y^\dagger_\beta] \tag{20}$$

is satisfied, the purely flavored CP asymmetry overshadows the lepton number violating piece, therefore leading to a regime where leptogenesis is entirely driven by flavor dynamics. In terms of scalar triplet interactions, this means that a purely flavored scalar triplet leptogenesis scenario naturally emerges whenever the triplets couple substantially less to SM scalars than to leptons, $B^\alpha_\phi \ll B^\alpha_\ell$ for at least one value of α. Note that although PFL scenarios in type-I seesaw can be defined as well, they differ significantly from the purely flavored scalar triplet leptogenesis scenario in that the latter just require suppressed lepton number violation in a single triplet generation i.e. suppression of lepton number breaking interactions in the full Lagrangian is not mandatory, as can be seen by noting that condition (20) can be satisfied even if $\mu_{\Delta_\alpha}/m_{\Delta_\alpha} \ll Y_\alpha$ for a single value of α.

We now turn to the case where the new states beyond the scalar triplet are RH neutrinos. In these scenarios the tree-level triplet decay involves only a vertex one-loop correction as shown in Fig. 2. The interference between the tree and one-loop level diagrams leads to the following CP asymmetry [14, 15]:

$$\epsilon^{\ell_i}_{\Delta} = -\frac{1}{4\pi}\sum_{\alpha,j} M_{N_\alpha}\frac{\mathbb{I}{\rm m}\left[\mu_\Delta Y^{ij}\lambda^*_{\alpha i}\lambda^*_{\alpha j}\right]}{m^2_\Delta {\rm Tr}[Y\,Y^\dagger]+|\mu_\Delta|^2}\ln\left(1+\frac{m^2_\Delta}{M^2_{N_\alpha}}\right) \ . \tag{21}$$

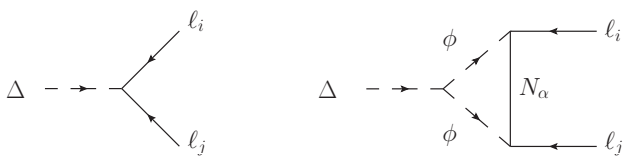

Figure 2: *Tree-level and one-loop Feynman diagrams accounting for the flavored CP asymmetry* $\epsilon^{\ell_i}_{\Delta_\alpha}$ *in scenarios featuring type-I and type-II interplay.*

Here the triplet generation index, being superfluous, has been dropped. In contrast to what has been found in the previous case, the resulting flavored CP asymmetry violates lepton flavor as well as lepton number. So, unless a specific (and somehow arbitrary) flavor alignment is assumed, so that $\sum_i \epsilon^{\ell_i}_{\Delta} = 0$, in these "hybrid" schemes PFL scenarios are not definable.

In the hierarchical case, $m_\Delta \ll M_{N_\alpha}$, the flavored CP asymmetry can be recasted in terms of triplet decay observables, namely

$$\epsilon^{\ell_i}_{\Delta} = \frac{1}{2\pi}\frac{m_\Delta}{v^2}\sqrt{B_\ell B_\phi}\frac{\mathbb{I}\mathrm{m}\left[\left(\mathcal{M}^\nu_\Delta \mathcal{M}^{\nu\dagger}_N\right)_{ii}\right]}{\tilde{m}_\Delta} \,, \tag{22}$$

with $\mathcal{M}^\nu_\Delta$ and $\mathcal{M}^\nu_N$ given by Eqs. (6) and (7). Note that in type-I+type-II scenarios, opposite to the scenario we consider here, it is also possible to generate the $B-L$ asymmetry from the decay of RH neutrinos via a vertex diagram involving a virtual scalar triplet, see in particular Refs. [14, 29, 30].

3 Boltzmann equations

In general, the evolution equations of particle asymmetries in the early Universe couple all particles species and thus involve a large number of reactions. However, a simplification is possible given that for specific temperature regimes different reactions have different timescales. Any reaction occurring in the heat bath will necessarily fall in one of the following categories[2]:

(I) Reactions which at a given temperature T_0 are much slower than the Hubble Universe expansion rate $H(T_0)$: $\Gamma_{\rm SR} \ll H(T_0)$.

(II) Reactions which at a given temperature T_0 are much faster than the Hubble Universe expansion rate $H(T_0)$: $\Gamma_{\rm FR} \gg H(T_0)$.

(III) Reactions which at a given temperature T_0 are comparable to the Hubble Universe expansion rate $H(T)$: $\Gamma_{\rm CR} \sim H(T_0)$.

[2]We thank Enrico Nardi for clarifying several aspects of this discussion.

At T_0, reactions falling in category I basically have not taken place, so they are of no relevance in the actual problem. The parameters responsible for such reactions can then be put to zero at the Lagrangian level, leading to the corresponding early Universe effective Lagrangian which involves new global symmetries implying new conservation laws [31]. In contrast, the reactions in II at T_0 have occurred so often that the particles involved attain thermodynamic equilibrium and so are subject to chemical equilibrium constraints, which enforce relations among the different particles chemical potentials (the particle asymmetries)[3]. These chemical equilibrium conditions, when coupled with the constraints implied by the conservation laws of the early Universe effective Lagrangian, allow to express the particle asymmetries of all the species in the thermal bath in terms of quasi-conserved charge asymmetries, the asymmetries related with charges that are only (slowly) broken by the reactions in III. Finally, reactions of type III are not fast enough to equilibrate the distributions of the intervening particles, and so they have to be accounted for via Boltzmann equations, which dictate the evolution of the quasi-conserved charge asymmetries and therefore of all the asymmetries in the heat bath. Note that for reactions of category I one has nevertheless to be cautious before dropping them from the Boltzmann equations. A well-known example, relevant in some cases for the dark matter abundance, is the freeze-in regime, i.e. slow production of dark matter particles from an out-of-equilibrium process [32]. Further on, in Sec. 4, we will see that in the PFL scenario a relatively similar effect, from very slow triplet interactions, can be relevant or even crucial, i.e. dominates the whole baryogenesis process (due to the fact that an additional asymmetry, the scalar triplet asymmetry, populates the heat bath, thus implying an additional Boltzmann equation).

The comparable-to-the-expansion triplet decays induce a $B-L$ ($B/3-L_i$ in the lepton flavored regime) and ϕ asymmetries. Although stemming from the same state and occurring at the same stage, these asymmetries follow different behaviors and so have to be treated in different ways. Let us discuss this in more detail. In the absence of triplet interactions, the full Lagrangian possesses a $U(1)_{B-L}$ symmetry no matter what the value of T_0 is. The $B-L$ charge asymmetry is therefore only affected by slow washouts (in that sense is a quasi-conserved charge) which implies that it is not entirely washed away and spreads all over the thermal bath feeding all the SM particle asymmetries. In the same token, the ϕ asymmetry is partially transferred to asymmetries in SM fermions through Yukawa interactions (those which at T_0 are in thermal equilibrium). However, while the evolution of the $B-L$ asymmetry is analyzed with the corresponding Boltzmann equations, the analysis of the evolution of the ϕ asymmetry does not require a Boltzmann equation: its evolution is determined by the chemical equilibrium conditions enforced by the reactions that at T_0 are in thermal equilibrium.

The network of Boltzmann equations for scalar triplet leptogenesis, no matter whether lepton flavor effects are active or not, corresponds to a system of coupled differential equations accounting for the temperature evolution of the triplet density $\Sigma_\alpha = \Delta_\alpha + \Delta_\alpha^\dagger$, the triplet asymmetry $\Delta_{\Delta_\alpha} = \Delta_\alpha - \Delta_\alpha^\dagger$ and the $B-L$ ($B/3-L_i$ in the lepton flavor regime)

[3]For a generic reaction $\sum_i X_i \rightleftharpoons \sum_i Y_i$ the chemical equilibrium condition read: $\sum_i \mu_{X_i} = \sum_i \mu_{Y_i}$, where μ_{X_i} and μ_{Y_i} are the chemical potentials of species X_i and Y_i.

charge asymmetry. The resulting network will of course—and unavoidably—involve the scalar doublet asymmetry, for which chemical equilibrium conditions have to be used in order to determine its dependence with the asymmetries that feed the heat bath (Δ_{Δ_α} and $B-L$), as it is done in the standard leptogenesis case [33, 34]. In what follows we will derive in detail the appropriate set of equations suitable for tackling the problem. We will closely follow the notation of [35].

In the hot plasma, triplets are subject to reactions that either tend to washout the $B-L$ asymmetry or to generate it. Depending on the interaction inducing the process one can distinguish—at tree-level—four kind of reactions: pure Yukawa, pure scalar, pure gauge and Yukawa-scalar reactions. Explicitly, for Δ_α, we have[4]:

- Yukawa and scalar-induced decay and inverse decays, $\Delta_\alpha \leftrightarrow \bar{\ell}\bar{\ell}$ and $\Delta_\alpha \leftrightarrow \phi\phi$, described by the reaction densities: $\gamma^{\ell}_{D_\alpha} \equiv \sum_{i,j} \gamma^{\Delta_\alpha}_{\ell_i\ell_j}$ and $\gamma^{\phi}_{D_\alpha} \equiv \gamma^{\Delta_\alpha}_{\phi\phi}$. The total decay reaction density thus given by $\gamma_{D_\alpha} = \gamma^{\ell}_{D_\alpha} + \gamma^{\phi}_{D_\alpha}$.

- Lepton flavor and lepton number ($\Delta L = 2$) violating Yukawa-scalar-induced and triplet-mediated s and t channel $2 \leftrightarrow 2$ scatterings $\phi\phi \leftrightarrow \bar{\ell}_i\bar{\ell}_j$ and $\phi\ell_j \leftrightarrow \bar{\phi}\bar{\ell}_i$, which are accounted for by the reaction densities $\gamma^{\phi\phi}_{\ell_i\ell_j}$ and $\gamma^{\phi\ell_j}_{\phi\ell_i}$.

- Lepton-flavor-violating Yukawa-induced and triplet-mediated s and t channel $2 \leftrightarrow 2$ scatterings: $\ell_n\ell_m \leftrightarrow \ell_i\ell_j$ and $\ell_j\ell_m \leftrightarrow \ell_i\ell_n$, with reaction densities given by $\gamma^{\ell_n\ell_m}_{\ell_i\ell_j}$ and $\gamma^{\ell_j\ell_m}_{\ell_i\ell_n}$.

- Gauge-induced $2 \leftrightarrow 2$ scatterings as follows: s-channel gauge-boson-mediated: $\Delta_\alpha\Delta_\alpha \leftrightarrow FF$ (F standing for SM fermions), $\Delta_\alpha\Delta_\alpha \leftrightarrow \phi\phi$ and $\Delta_\alpha\Delta_\alpha \leftrightarrow VV$ (V standing for SM gauge bosons); t and u channel triplet-mediated: $\Delta_\alpha\Delta_\alpha \leftrightarrow VV$ and four-point vertex $\Delta_\alpha\Delta_\alpha \leftrightarrow VV$ reactions. All together they are characterized by the reaction density γ_{A_α}.

Note that if the flavor degrees of freedom were to be neglected, all the reactions—apart from those in the third item—would still be present in their unflavored form. The reactions in third item are therefore inherent to scalar flavored leptogenesis.

All together, these reactions lead to the following network of flavored classical Boltzmann equations[5]:

$$\dot{Y}_{\Delta_{\Delta_\alpha}} = -\left[\frac{Y_{\Delta_{\Delta_\alpha}}}{Y^{\rm Eq}_{\Sigma}} - \sum_k \left(\sum_i B^{\alpha}_{\ell_i} C^{\ell}_{ik} - B^{\alpha}_{\phi} C^{\phi}_{k}\right) \frac{Y_{\Delta_k}}{Y^{\rm Eq}_{\ell}}\right] \gamma_{D_\alpha} \ , \tag{23}$$

$$\dot{Y}_{\Sigma_\alpha} = -\left(\frac{Y_{\Sigma_\alpha}}{Y^{\rm Eq}_{\Sigma}} - 1\right) \gamma_{D_\alpha} - 2\left[\left(\frac{Y_{\Sigma_\alpha}}{Y^{\rm Eq}_{\Sigma}}\right)^2 - 1\right] \gamma_{A_\alpha} \ , \tag{24}$$

[4]Expressions for all the intervening reaction densities can be found in Appx. A.

[5]This network of equations turns out to be consistent and suitable if one aims to study the generation of the $B-L$ asymmetry in the fully flavored regime, where lepton flavor decoherence is fully accomplished. If instead one aims to analyze the problem in transition regimes, a treatment based on the density matrix formalism will be required, as has been discussed e.g. in [36].

$$\dot{Y}_{\Delta_{B/3-L_i}} = -\left(\frac{Y_{\Sigma_\alpha}}{Y_\Sigma^{\rm Eq}}-1\right)\epsilon^{\ell_i}_{\Delta_\alpha}\gamma_{D_\alpha} + 2\sum_j\left(\frac{Y_{\Delta_{\Delta_\alpha}}}{Y_\Sigma^{\rm Eq}} - \frac{1}{2}\sum_k C^\ell_{ijk}\frac{Y_{\Delta_k}}{Y_\ell^{\rm Eq}}\right)B^\alpha_{\ell_{ij}}\gamma_{D_\alpha}$$
$$- 2\sum_{j,k}\left(C^\phi_k + \frac{1}{2}C^\ell_{ijk}\right)\frac{Y_{\Delta_k}}{Y_\ell^{\rm Eq}}\left(\gamma'^{\phi\phi}_{\ell_i\ell_j} + \gamma^{\phi\ell_j}_{\phi\ell_i}\right) - \sum_{j,m,n,k} C^\ell_{ijmnk}\frac{Y_{\Delta_k}}{Y_\ell^{\rm Eq}}\left(\gamma'^{\ell_n\ell_m}_{\ell_i\ell_j} + \gamma^{\ell_m\ell_j}_{\ell_i\ell_n}\right) \ . \tag{25}$$

Here we have adopted the following conventions (details can be found in Appx. A). A fraction of the asymmetry generated in ℓ_i is transferred to RH charged leptons, e_i, via SM Yukawa interactions, and so $L_i = 2\ell_i + e_i$. We use the particle number density-to-entropy ratio defined as $Y_{\Delta_X} = \Delta n_X/s = (n_X - n_{\bar{X}})/s$, where n_X ($n_{\bar{X}}$) is the number density of species X ($\bar{X}$) and s is the entropy density. We have defined $Y_{\Delta_\Delta} \equiv Y_{\Delta_{\Delta^0}} = Y_{\Delta_{\Delta^+}} = Y_{\Delta_{\Delta^{++}}}$ and $Y_{\Delta_\phi} \equiv Y_{\Delta_{\phi^0}} = Y_{\Delta_{\phi^+}}$. The derivative is denoted according to $\dot{Y} \equiv sHz_\alpha dY/dz_\alpha$, with H the expansion rate of the Universe, and as usual $z_\alpha = m_{\Delta_\alpha}/T$. Primed s-channel scattering reaction densities refer to the rates with resonant intermediate state subtracted: $\gamma' = \gamma - \gamma^{\text{on-shell}}$. Finally the matrices C^ℓ_{ijk} and C^ℓ_{ijmnk} are defined according to

$$\begin{aligned} C^\ell_{ijk} &= C^\ell_{ik} + C^\ell_{jk} \ , \\ C^\ell_{ijmnk} &= C^\ell_{ik} + C^\ell_{jk} - C^\ell_{mk} - C^\ell_{nk} \ , \end{aligned} \tag{26}$$

where the C^ℓ and C^ϕ matrices (*asymmetry coupling matrices*) relate the asymmetry in lepton and scalar doublets with the $B/3-L_k$ and triplet asymmetries—the "fundamental" asymmetries present in the plasma—according to

$$Y_{\Delta_{\ell_i}} = -\sum_k C^\ell_{ik}\, Y_{\Delta_k} \qquad \text{and} \qquad Y_{\Delta_\phi} = -\sum_k C^\phi_k\, Y_{\Delta_k} \ . \tag{27}$$

In these relations the asymmetries Y_{Δ_k} are given by the components of the asymmetry vector

$$\vec{Y}_\Delta = \begin{pmatrix} Y_{\Delta_\Delta} \\ Y_{\Delta_{B/3-L_k}} \end{pmatrix} \ , \tag{28}$$

and the structure of the C^ℓ and C^ϕ *asymmetry coupling matrices* becomes determined by the constraints coming from the global symmetries of the effective Lagrangian and the chemical equilibrium conditions enforced by those SM reactions which in the relevant temperature regime (the regime at which the $B-L$ asymmetry is generated) are faster than the Universe Hubble expansion rate. The final baryon asymmetry is then given by

$$Y_{\Delta_B} = 3 \times \frac{12}{37}\sum_i Y_{\Delta_{B/3-L_i}} \ , \tag{29}$$

where the factor 3 accounts for the different $SU(2)$ degrees of freedom of the scalar triplet.

Before discussing chemical equilibration, we also write Boltzmann equations valid in the case where the top Yukawa-related reactions are either the only fast Yukawa processes ($10^{12}\,\text{GeV} \lesssim T \lesssim 10^{15}\,\text{GeV}$) or slow ($T \gtrsim 10^{15}\,\text{GeV}$), or when quantum lepton flavor

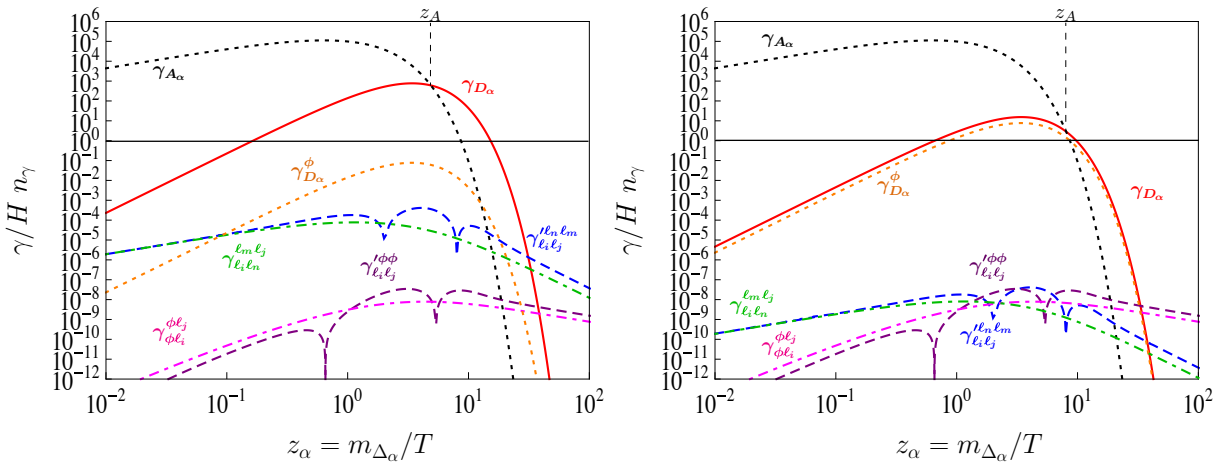

Figure 3: *Reaction densities for the different processes involved in scalar triplet flavored leptogenesis. In the left-hand side plot* $B_\phi = 10^{-4}$ *while in the right-hand side plot* $B_\phi = B_\ell = 0.5$ *(*$B_\ell = 1 - B_\phi$*). The remaining parameters have been fixed according to* $m_{\Delta_\alpha} = 10^9\, GeV$ *and* $\tilde{m}_{\Delta_\alpha} = 10^{-2}\, eV$.

coherence is already broken but an alignment in lepton flavor space is fixed (i.e. Δ couples to only one flavor combination). We will refer these cases as "the one lepton flavor approximation" (see Appx. B.2 for further details). In addition to Eq. (24) which holds no matter the regime, one has

$$\dot{Y}_{\Delta_{\Delta_\alpha}} = -\left[\frac{Y_{\Delta_{\Delta_\alpha}}}{Y_\Sigma^{\rm Eq}} - \sum_k \left(B_\ell^\alpha C_k^\ell - B_\phi^\alpha C_k^\phi\right)\frac{Y_{\Delta_k}}{Y_\ell^{\rm Eq}}\right]\gamma_{D_\alpha}\ , \tag{30}$$

$$\dot{Y}_{\Delta_{B-L}} = -\left(\frac{Y_{\Sigma_\alpha}}{Y_\Sigma^{\rm Eq}} - 1\right)\epsilon_{\Delta_\alpha}\gamma_{D_\alpha} + 2\left(\frac{Y_{\Delta_{\Delta_\alpha}}}{Y_\Sigma^{\rm Eq}} - \sum_k C_k^\ell \frac{Y_{\Delta_k}}{Y_\ell^{\rm Eq}}\right)B_\ell^\alpha \gamma_{D_\alpha}$$
$$- 2\sum_k \left(C_k^\phi + C_k^\ell\right)\frac{Y_{\Delta_k}}{Y_\ell^{\rm Eq}}\left(\gamma^{\prime\phi\phi}_{\ell\ell} + \gamma^{\phi\ell}_{\phi\ell}\right)\ , \tag{31}$$

where in this case the asymmetry vector is reduced to $\vec{Y}_\Delta^T = (Y_{\Delta_\Delta}, Y_{\Delta_{B-L}})$, and so the relation between the lepton doublet asymmetry and $\vec{Y}_\Delta$ reads like in (27), dropping the lepton flavor index. Note that the evolution equations derived in Ref. [15] match with (30)-(31) provided in the latter all SM Yukawa interactions effects are neglected, see Eq. (38) below.

A final comment before we proceed with the following section. A quite accurate calculation of the resulting $B - L$ asymmetry can be done by considering only decays, inverse decays, gauge induced reactions and the off-shell pieces of the s-channel processes: $\gamma^{\prime\phi\phi}_{\ell_i\ell_j}$ and $\gamma^{\prime\ell_n\ell_m}_{\ell_i\ell_j}$, which guarantee that the resulting equations have a consistent thermodynamic behavior. This is demonstrated by Fig. 3 where we have plotted the different reaction densities as a function of z_α by fixing the relevant parameters according to $m_{\Delta_\alpha} = 10^9\,$GeV, $\tilde{m}_{\Delta_\alpha} = 10^{-2}$ eV and $B_\phi^\alpha = 10^{-4}$ ($B_\phi^\alpha = 0.5$) for the plot on the left (right). Thus, from

now on and throughout the numerical calculation we will drop the third and fourth term in Eq. (25). In the network of unflavored kinetic equations such approximation implies dropping the third term in Eq. (31).

3.1 Chemical equilibrium conditions

At very high temperatures ($T \gtrsim 10^{15}$ GeV) all SM reactions are frozen in the sense of item I. As the temperature drops, certain reactions (those driven by the largest couplings first) attain thermal equilibrium which demands kinetic as well as chemical equilibrium of the corresponding reactions, the latter in turn enforce constraints among the different chemical potentials of the intervening particles. Since for a relativistic species X the particle number density-to-entropy ratio is, at leading order in μ/T, related with the chemical potential according to [37]:

$$Y_{\Delta_X} = \frac{T^2}{6s}\, g_X\, \mu_X \begin{cases} 1\ , & \text{for fermions} \\ 2\ , & \text{for bosons}\ , \end{cases} \tag{32}$$

(with g_X the number of degrees of freedom[6]) the chemical equilibrium constraints thus relate the different particle asymmetries of those species participating in fast reactions.

In principle, there is a chemical potential (an asymmetry) for each particle in the thermal bath, which implies that *a priori* there are as many chemical potentials as particles in the plasma: 61. This number, however, is largely reduced due to the constraints imposed by the set of chemical equilibrium conditions and the conservation laws of the early Universe effective Lagrangian. Depending on the temperature regime where the $B-L$ asymmetry is generated, the possible constraints on the chemical potentials are:

1. Chemical potentials for gauge bosons vanish $\mu_{W^i} = \mu_{\mathcal{B}} = \mu_g = 0$, and so the components of the electroweak and color multiplets have the same chemical potentials [37]. This already reduces to 17 the number of independent asymmetries.

2. Regardless of the temperature regime, cosmological hypercharge neutrality must be obeyed, namely

$$\mathcal{Y} = \sum_i \left(\mu_{Q_i} + 2\mu_{u_i} - \mu_{d_i} - \mu_{\ell_i} - \mu_{e_i} + 2\mu_\phi + 6\mu_\Delta\right) = 0\ . \tag{33}$$

3. Non-perturbative QCD instanton and electroweak sphaleron reactions—if in thermal equilibrium—enforce the following constraints:

$$\sum_i \left(2\mu_{Q_i} - \mu_{u_i} - \mu_{d_i}\right) = 0\ , \qquad \sum_i \left(3\mu_{Q_i} + \mu_{\ell_i}\right) = 0\ . \tag{34}$$

   The temperature at which the QCD instanton reactions attain equilibrium has been estimated to be $T \sim 10^{13}$ GeV [38, 39] while for electroweak sphaleron processes, being

[6] Using our previous definitions, we have $g_\Delta = g_\phi = g_{Q_i} = g_{u_i} = g_{d_i} = g_{\ell_i} = g_{e_i} = 1$.

controlled by α_{EW} rather than α_S, it has been found to be about a factor 20 smaller [39].

4. Finally Yukawa reactions when being in thermal equilibrium lead to the chemical equilibrium constraints:

$$\text{Up-type quarks:} \qquad \mu_{u_i} - \mu_{Q_i} - \mu_\phi = 0 \ , \tag{35}$$

$$\text{Down-type quarks:} \qquad \mu_{d_i} - \mu_{Q_i} + \mu_\phi = 0 \ , \tag{36}$$

$$\text{Charged leptons:} \qquad \mu_{e_i} - \mu_{\ell_i} + \mu_\phi = 0 \ . \tag{37}$$

Top Yukawa-induced reactions are in thermodynamic equilibrium for $T \lesssim 10^{15}$ GeV. Bottom, charm and tau Yukawa-induced processes are in equilibrium at $T \lesssim 10^{12}$ GeV, strange and muon at $T \lesssim 10^9$ GeV, and the first generation Yukawa-induced processes at $T \lesssim 10^5$ GeV [36, 40, 42].

The exact number of non-vanishing chemical potentials as well as the number of chemical equilibrium conditions are fixed only when a specific temperature window is settled. Once this is done, the resulting system of equations is solved in terms of a single set of variables, which we take to be $\mu_{B/3-L_i}$ and μ_Δ. The solution thus provides the relations between the asymmetries of all the particles in the heat bath with the independent asymmetries $\{Y_\Delta\} = \{Y_{\Delta_\Delta}, Y_{B/3-L_i}\}$ appearing in the asymmetry vector in (28).

In what follows we briefly discuss the symmetries of the corresponding early Universe effective Lagrangian and the relevant chemical equilibrium conditions in 1-4 which enable us to calculate the rectangular matrices relating the lepton and scalar doublet asymmetries with $\{Y_\Delta\}$, as given by Eqs. (27). In each regime, when applicable, we also discuss in Appx. B.2 the one-flavor limit by taking flavor alignments as in Ref. [34] and deriving the corresponding $C^{\ell,\phi}$ matrices needed in such approximations. We start by discussing the high temperature regime $T > 10^{15}$ GeV, proceeding subsequently to the temperature ranges $T \subset [10^{12}, 10^{15}]$ GeV, $[10^9, 10^{12}]$ GeV, $[10^5, 10^9]$ GeV and $T < 10^5$ GeV. Theses ranges are based on the assumption that all SM interactions that approximately enter in thermal equilibrium at a similar temperature do it effectively at the same temperature. We stress that some of these temperature "windows" differ from those used in Ref. [40], in particular in what regards the charged lepton Yukawa reaction equilibrium temperatures. They however match with those pointed out in Ref. [36].

- *None SM reactions in thermal equilibrium, $T \gtrsim 10^{15}$ GeV*:
  In this regime all SM reactions are slow in the sense of I, and so only triplet-related interactions are relevant. A proper treatment of the problem therefore should be done with the unflavored kinetic equations in (24), (30) and (31), bearing in mind that since in the heat bath the triplet is subject only to scalar- and Yukawa-induced interactions, in Eq. (24) the second term can be neglected. With all SM reactions frozen, only the triplet, lepton and scalar doublets develop chemical potentials: μ_Δ, μ_ℓ, μ_ϕ. These chemical potentials are subject only to the hypercharge neutrality constraint in 2, which leads to the following C^ℓ and C^ϕ matrices:

$$C^\ell = \begin{pmatrix} 0 & 1/2 \end{pmatrix} \ , \qquad C^\phi = \begin{pmatrix} 3 & 1/2 \end{pmatrix} \ . \tag{38}$$

The resulting Boltzmann equations match those derived in Refs. [11, 15] since there, regardless of the temperature considered, no SM Yukawa interactions effects were taken into account, neither from the quarks nor from the charged leptons. Strictly speaking, this is an accurate procedure only in this regime, $T \gtrsim 10^{15}$ GeV, given that none of the SM Yukawa reactions are in thermal equilibrium (from now on, when necessary we will refer to this literature-reference-scheme as the "unflavored case"). It is worth stressing that through Eq. (27) the C^{ϕ} matrix in Eq. (38) leads to the sum rule:

$$6Y_{\Delta_\Delta} + 2Y_{\Delta_\phi} + Y_{\Delta_{B-L}} = 0\,. \tag{39}$$

This expression is nothing else but the sum rule employed in Ref. [15] (taking into account the fact that, in this reference, Y_{Δ_Δ} and Y_{Δ_ϕ} involve a sum on the $SU(2)$ degrees of freedom, so that one must substitute $Y_{\Delta_\Delta} \to 3Y_{\Delta_\Delta}$ and $Y_{\Delta_\phi} \to 2Y_{\Delta_\phi}$). Note that above 10^{15} GeV there is relatively little time for the reheating to occur before the temperature goes below the scalar triplet mass (assuming the reheating occurs below the Planck scale). So, unless the triplet Yukawa couplings are such that at $T \sim m_\Delta$ the triplet still follows a thermal distribution (strong washout regime), the final baryon asymmetry produced will depend on the initial scalar triplet number density (initial condition), i.e. will further depend on the details of the reheating. We will not consider these possible effects here. Note also that above 10^{15} GeV, for $\tilde{m}_\Delta \sim 0.05$ eV one gets non perturbative Yukawa couplings if $B_\phi \lesssim 8 \cdot 10^{-3}$.

- *Only top Yukawa-related reactions in thermal equilibrium, $T \subset [10^{12}, 10^{15}]$ GeV*:
  Within this temperature regime, apart from top Yukawa-related interactions which are fast, all SM Yukawa-induced reactions fall in category I. Accordingly, the correct description of the problem is given by the one lepton flavor approximation equations in (24), (30) and (31).

  The global symmetries of the effective Lagrangian are those of the SM kinetic terms broken only by the top Yukawa coupling, and so the group of global transformations is:

  $$G_{\rm Eff} = U(1)_Y \times U(1)_B \times U(1)_e \times U(1)_{\rm PQ} \times SU(3)_d \times SU(3)_e \times SU(2)_Q \times SU(2)_u\,. \tag{40}$$

  The $SU(3)$ factors combined with the exact $U(1)_B$, $U(1)_{\rm PQ}$ and the absence of Yukawa couplings for all SM particles, except the top quark, imply: $\mu_{d_i} = \mu_{e_i} = \mu_{u_{1,2}} = \mu_{Q_{1,2}} = \mu_B = 0$. Taking this constraints into account and the relevant chemical equilibrium conditions (33) and (35), the latter written only for the top quark, we obtain

  $$C^{\ell} = \begin{pmatrix} 0 & 1/2 \end{pmatrix}\,, \qquad C^{\phi} = \begin{pmatrix} 2 & 1/3 \end{pmatrix}\,. \tag{41}$$

  Including these effects will enhance the efficiency by about 20% with respect to the unflavored case, the precise value being of course dependent upon the parameter choice.

- *QCD instantons, electroweak sphalerons, bottom, charm and tau Yukawa-related reactions in thermal equilibrium, $T \subset [10^9, 10^{12}]$ GeV*:

In this temperature window the lepton doublets lose their quantum coherence due to the tau Yukawa-related interactions being in thermal equilibrium [40, 42]. On the other hand, since electroweak sphaleron reactions are in thermal equilibrium, baryon number is no longer conserved, while they conserve the individual $B/3 - L_i$ charges. An appropriate study of the evolution of the $B - L$ asymmetry should then be done by tracking the evolution of the flavored charge asymmetries $B/3 - L_i$ ($i = a, \tau$, the state a being a coherent superposition of e and μ lepton flavors) with the network of Eqs. (23)-(25).

The QCD instantons reactions break the global $U(1)_{\rm PQ}$, the bottom and tau Yukawa couplings break the RH down-type quark and charged lepton $SU(3)$ flavor multiplet and in addition the tau Yukawa coupling also breaks the global $U(1)_e$. The Lagrangian is as expected "less symmetric", with the group of global transformations given by

$$G_{\rm Eff} = U(1)_Y \times SU(2)_d \times SU(2)_e \times U(1)_Q \times U(1)_u \ . \tag{42}$$

These global symmetries imply: $\mu_{u_1} = \mu_{Q_1} = 0$ and $\mu_{d_i} = \mu_{e_i} = 0$ with $i = 1, 2$, while the complete set of chemical equilibrium conditions correspond to (33) for hypercharge neutrality (written so to include the now non-vanishing bottom, charm and tau chemical potentials), (34) for QCD instantons, (34) for electroweak sphalerons, and (35), (36) and (37) written for top, bottom,charm and tau Yukawa interactions. Due to sphaleron reactions, lepton flavor is no longer conserved so that chemical potentials develop in three independent lepton doublets: ℓ_τ, ℓ_a and ℓ_b. Conservation of the $B/3 - L_i$ charges however provide the constraint $\mu_{B/3-L_b} = 0$, which when coupled with the corresponding chemical equilibrium conditions yields the following flavored $C^{\ell,\phi}$ matrices:

$$C^\ell = \begin{pmatrix} -6/359 & 307/718 & -18/359 \\ 39/359 & -21/718 & 117/359 \end{pmatrix} \ , \quad C^\phi = \begin{pmatrix} 258/359 & 41/359 & 56/359 \end{pmatrix} \ . \tag{43}$$

- *Strange and muon Yukawa interactions in thermal equilibrium, $T \subset [10^5, 10^9]$ GeV:* As pointed out in Ref. [40, 42], in this temperature regime the lepton doublets completely lose their quantum coherence, implying that chemical potentials develop in each orthogonal lepton flavor doublet: ℓ_τ, ℓ_μ and ℓ_e. Since the second generation Yukawa reactions are no longer of type I, the symmetries of the effective Lagrangian are reduced to $U(1)$ factors:

$$G_{\rm Eff} = U(1)_Y \times U(1)_d \times U(1)_e \times U(1)_Q \times U(1)_u \ . \tag{44}$$

These constraints imply $\mu_d = \mu_e = \mu_{Q_1} = \mu_u = 0$, and when combined with the corresponding chemical equilibrium conditions (the ones from previous item complemented with (35), (36) and (37) for the charm, strange and muon Yukawa

interactions) yield:

$$C^{\ell} = \begin{pmatrix} -6/179 & 151/358 & -10/179 & -10/179 \\ 33/358 & -25/716 & 172/537 & -7/537 \\ 33/358 & -25/716 & -7/537 & 172/537 \end{pmatrix} , \tag{45}$$

$$C^{\phi} = \begin{pmatrix} 123/179 & 37/358 & 26/179 & 26/179 \end{pmatrix} . \tag{46}$$

- *All SM reactions in thermal equilibrium, $T \lesssim 10^5$ GeV:*
  In this case and until electroweak symmetry breaking, the only surviving symmetry is $U(1)_Y$. Due to all SM reactions being fast, all SM particles develop non-vanishing chemical potentials, with the chemical equilibrium conditions given by the full list in items 1-4. The flavored $C^{\ell,\phi}$ rectangular matrices in this regime therefore read:

$$C^{\ell} = \begin{pmatrix} 9/158 & 221/711 & -16/711 & -16/711 \\ 9/158 & -16/711 & 221/711 & -16/711 \\ 9/158 & -16/711 & -16/711 & 221/711 \end{pmatrix} , \tag{47}$$

$$C^{\phi} = \begin{pmatrix} 39/79 & 8/79 & 8/79 & 8/79 \end{pmatrix} . \tag{48}$$

3.2 Domain of validity of the various sets of flavored Boltzmann equations

The temperature ranges discussed in the previous Sec. are determined from the assumption that lepton flavor decoherence happens as soon as the corresponding lepton Yukawa interaction rate becomes faster than the Hubble rate, at a temperature $T \equiv T_h$. Lepton flavor decoherence is a delicate issue which requires a pure quantum treatment, which in full generality does not even exist for the more widely considered *standard* leptogenesis picture. Here, in this Sec. rather than providing an exhaustive treatment of this issue, we will consider a simplified treatment considering the two most relevant processes: SM lepton Yukawa reactions (given approximately by Eq. (102)) and lepton-related triplet inverse decays, basically along the lines of Ref. [41].

If at the time when a lepton Yukawa interaction rate becomes faster than the Hubble rate, the triplet inverse decay processes $\ell\ell \to \bar{\Delta}$ are much faster than this reaction, the coherent superposition of leptons produced from the decay of a scalar triplet will inverse decay before it has the time to undergo any red charged lepton Yukawa interaction. In this case it is expected that decoherence is fully achieved only later when the inverse decay rate, which is Boltzmann suppressed at low temperatures, gets smaller than the SM lepton Yukawa rate, at a temperature $T \equiv T_{\rm decoh}$. Between T_h and $T_{\rm decoh}$, one lies in an intermediate regime where flavor effects are suppressed.

The parameters which determine $T_{\rm decoh}$ are m_Δ and the inverse leptonic decay effective parameter:

$$\tilde{m}_\Delta^{\rm eff} \equiv \tilde{m}_\Delta \sqrt{\frac{1 - B_\phi}{B_\phi}} . \tag{49}$$

Imposing that the lepton-related triplet inverse decays never get faster than a given SM Yukawa reaction at a given temperature, one can derive upper bounds on the triplet mass as a function of $\tilde{m}_\Delta^{\rm eff}$, in the same way it has been done in the type-I seesaw case [41]. These bounds are shown in the left-hand side plot in Fig. 4, with the constraints applying in the tau (muon) case displayed in solid red (orange) line, labeled by "fully 2(3)-flavor". Analytically the bounds are given by the requirement that

$$\Gamma_{f_i} \gtrsim B_\ell \, \Gamma_\Delta^{\rm Tot} \frac{Y_\Sigma^{\rm Eq}}{Y_\ell^{\rm Eq}} \qquad (f_i = \tau, \mu) \ , \tag{50}$$

where $B_\ell \, \Gamma_\Delta^{\rm Tot} \propto \tilde{m}_\Delta^{\rm eff}$ (see Eq. (10)) and where the corresponding SM reaction rates are given by γ_{f_i}/n_{f_i}, with γ_{f_i} approximately given by Eq. (102). The constraints in (50) then translate into constraints over m_Δ and $\tilde{m}_\Delta^{\rm eff}$, and fix the values that these parameters should have in order to assure that triplet dynamics takes place in either a "fully" two or three flavor regime, namely

$$m_\Delta \lesssim 4 \times \left(\frac{10^{-3}{\rm eV}}{\tilde{m}_\Delta^{\rm eff}} \right) \times 10^{11} \ {\rm GeV} \qquad \text{fully 2-flavor regime;} \tag{51}$$

$$m_\Delta \lesssim 1 \times \left(\frac{10^{-3} \ {\rm eV}}{\tilde{m}_\Delta^{\rm eff}} \right) \times 10^{9} \ {\rm GeV} \qquad \text{fully 3-flavor regime.} \tag{52}$$

For illustration we take the example of the decoherence effect associated with the τ SM Yukawa interaction. If below the temperature $T = T_h^\tau \simeq 10^{12}$ GeV (at which the τ Yukawa rate gets faster than the Hubble rate) the $\ell\ell \to \bar{\Delta}$ inverse decay rate is slower than this Yukawa rate, one enters in the 2 flavor regime defined by Eqs. (42) already at $T = T_h^\tau$. For example, for $B_\phi = 0.5$ and $\tilde{m}_\Delta \simeq 10^{-3}$ eV which gives $\tilde{m}_\Delta^{\rm eff} = 10^{-3}$ eV, one trivially satisfies the condition in Eq. (51) for any mass since in this case triplet inverse decays never reach thermal equilibrium. On the contrary, if $\tilde{m}_\Delta^{\rm eff} \gtrsim 10^{-3}$ eV the triplet inverse decay rate is faster than the τ Yukawa rate down to a smaller temperature, $T_{\rm decoh}^\tau \lesssim T_h^\tau$. In this case one can use the network of flavored Boltzmann equations in (23)-(25), written in the two-flavor regime, only below $T_{\rm decoh}^\tau$. Fig. 4 (right-hand plot), which shows the dependence of $T_{\rm decoh} = m_\Delta/z_{\rm decoh}$ (for tau and muon reactions displayed in red and orange colors respectively) with the triplet mass for several values of $\tilde{m}_\Delta^{\rm eff}$ (solid-dashed-dotted: 10^{-2}-1-10^2 eV), proves that for large values of $\tilde{m}_\Delta^{\rm eff}$—not satisfying the lower limit given by Eq. (51)—this temperature can be far below 10^{12} GeV.

In more detail, taking $m_\Delta = 10^{10}$ GeV, $\tilde{m}_\Delta = 0.01$ eV and $B_\phi = 10^{-4}$, which gives $\tilde{m}_\Delta^{\rm eff} \approx 1$ eV, one gets $T_{\rm decoh}^\tau \simeq 10^9$ GeV. Above $T_{\rm decoh}^\tau$ one expects the decoherence effect to be mild, so that for 10^9 GeV $\lesssim T \lesssim 10^{12}$ GeV and for this parameter choice one should better use a set of Boltzmann equations where the QCD and electroweak instantons as well as the top, bottom and charm Yukawa interactions are all in thermal equilibrium but the τ Yukawa is still effectively "off" for what concerns the $B - L$ asymmetry production process (even if faster than the Hubble rate). Therefore within this temperature range, and for this parameter choice, one has still a single lepton flavour Boltzmann equation

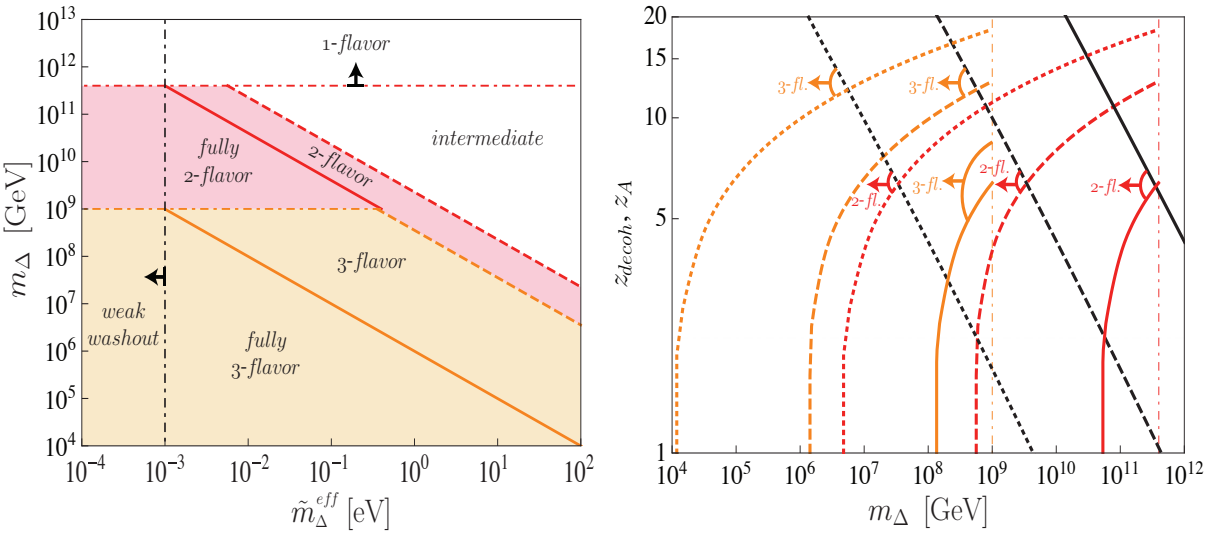

Figure 4: *Left: regions determining the different flavor regimes as a function of* $\tilde{m}_\Delta^{eff}$ *and* m_Δ*. The region below the red (orange) solid line is obtained by the requirement that the* $\tau(\mu)$ *Yukawa rate is always faster than the* $\ell\ell \to \bar{\Delta}$ *inverse decay rate, determining the fully 2(3)-flavors regime. The region below the red (orange) dashed line is obtained by the requirement that the* $\tau(\mu)$ *Yukawa rate is faster than the* $\ell\ell \to \bar{\Delta}$ *inverse decay rate for* $z \geq z_A$ *(see the right plot). The red (orange) horizontal dot-dashed line corresponds to the value of* m_Δ *above which the* $\tau(\mu)$ *Yukawa never reach thermal equilibrium. The vertical dot-dashed line corresponds to the value of* $\tilde{m}_\Delta^{eff}$ *below which inverse decays never reach thermal equilibrium. Right:* z^τ_{decoh} *(red),* z^μ_{decoh} *(orange) and* z_A *(black) as a function of* m_Δ*, for* $\tilde{m}_\Delta^{eff} = 0.01$ *eV (solid), 1 eV (dashed) and 100 eV (dotted), where* $z_{decoh} = m_\Delta/T_{decoh}$ *and* $z_A = m_\Delta/T_A$*. The vertical red (orange) dot-dashed line corresponds to the value of* m_Δ *above which the* $\tau(\mu)$ *Yukawa never reach thermal equilibrium. As explained in the text, for* $z \leq z^\tau_{decoh}$ *(*$z > z^\tau_{decoh}$*), the 1(2)-flavor Boltzmann equations must be used (and similarly for* z^μ_{decoh} *with 2(3)-flavors). On the other hand, the* z_A *lines determine when the use of a simple set of Boltzmann equations for all* z *gives a reliable result. Since the asymmetry is mainly produced when* $z > z_A$*, if* $z_A > z^\tau_{decoh}$ *(*$z_A > z^\mu_{decoh}$*) it is indeed a good approximation to use a 2(3)-flavor Boltzmann equation set for all* z*.*

with C^ℓ and C^ϕ matrices which take into account the effects of all these instantons and t, b ,c Yukawa interactions

$$C^\ell = \begin{pmatrix} 0 & 3/10 \end{pmatrix} \qquad C^\phi = \begin{pmatrix} 3/4 & 1/8 \end{pmatrix} \tag{53}$$

In other words in this case, one does not consider the chemical potential relation associated to the τ Yukawa interaction even if the corresponding rate is faster than the Hubble rate. Strictly speaking this relation holds for an infinitely fast reaction rate. Here the rate is slower than the inverse decay rate (closely related to the $B-L$ asymmetry production) and cannot be considered as infinitely fast. To sum up, within the $10^{12}-10^9$ GeV range, strongly depending on parameter configurations (m_Δ and $\tilde{m}_\Delta^{\rm eff}$), one has two possible sets of C^ℓ and C^ϕ matrices, thus implying that the problem of tracking the evolution of the $B-L$ asymmetry is described either by the kinetic equations given in Eqs (30)-(31) with C^ℓ and C^ϕ matrices given by Eq. (53) if $T > T^\tau_{\rm decoh}$, either by the kinetic equations given in (23)-(25) with C^ℓ and C^ϕ matrices given by Eq. (43) whenever $T < T^\tau_{\rm decoh}$.

As for the next temperature range, between $T_h^\mu \simeq 10^9$ GeV and $T_h^e \simeq 10^5$ GeV, where both the s and the μ rate are also faster than the Hubble rate, there one has three possible regimes: (i) the one-flavor case, as long as the τ is "off" (if still it is, which implies that the μ Yukawa "off" too); (ii) the two-lepton-flavor case when the τ is "on" but the μ Yukawa is still "off"; (iii) the three-flavor case discussed in the previous Sec. when both the τ and μ Yukawas are "on", and for which the C^ℓ and C^ϕ matrices are given by Eq. (45). Finally below 10^5 GeV where the up, down and electron Yukawa interaction rates are faster than the Hubble rate, one has 4 situations depending on which interactions are "off": (i) τ, μ, e "off" (one flavor), (ii) μ, e "off" (2 flavors), (iii) e "off" (3 flavors) and (iv) all interactions "on" (3 flavors). Apart from case (iv), for which the C^ℓ and C^ϕ matrices are given in Eqs. (47) and (48), the corresponding sets of C^ℓ and C^ϕ matrices for the remaining situations are given in Appx. B.1. The temperature ranges where they hold are given in the right panel of Fig. 4, for μ and τ only for the sake of clarity.

For the cases where one would have several sets of Boltzmann equations to take into account successively as the temperature goes down, one important remark to be done is that the transition between these regimes might be non-trivial to treat in a satisfactory way. Just assuming a step function in temperature from one regime to the next one could easily constitute a too rough procedure. In the following we will not consider such kind of cases. In fact in many situations this question turns out to be of little numerical importance.

In the type-I case, basically this is of no numerical importance if the inverse decays have never been faster than the lepton Yukawa rate [41], a condition which in the type-II case gives Eq. (51). However, for the type-II case this condition turns out to be too conservative. The difference comes from the fact that the scalar triplets, unlike right-handed neutrinos, have gauge interactions. As explained in detail in e.g. Ref. [11, 15], see also section 5 below, this implies that as long as the gauge scattering rate is faster than the decay rate, scalar triplets gauge scatter before they have the time to decay, and the asymmetry production is highly suppressed. Only from the temperature "T_A" where the gauge scattering rate gets smaller than the decay rate, a substantial asymmetry can

develop itself. This means that if $T_{\rm decoh} \gtrsim T_A$, all what happens at $T > T_{\rm decoh}$ is anyway irrelevant and one can safely use only the set of Boltzmann equations where decoherence is assumed. If instead $T_{\rm decoh} \ll T_A$ the asymmetry produced for $T < T_{\rm decoh}$ will be suppressed from the fact that the number of triplets remaining at $T \sim T_{\rm decoh}$ is Boltzmann suppressed. In this case one expects the unflavored period to dominate the production of the asymmetry, as the number of triplets still present at $T \simeq T_A$ is larger. This means that for the PFL case to be discussed in Sec. 4, where there is no asymmetry production in the unflavored regime, better $T_{\rm decoh} \gtrsim T_A$.

In practice the condition $T_{\rm decoh} \gtrsim T_A$ is much less restrictive than Eq. (51). In the right panel of Fig. 4, we plotted in black the values of $z_A = m_\Delta/T_A$ red for different values of $\tilde{m}_\Delta^{\rm eff}$. For example, if $\tilde{m}_\Delta^{\rm eff} = 1$ eV, one observes that $T^\tau_{\rm decoh} \gtrsim T_A$ requires $m_\Delta \lesssim 10^9$ GeV, while if $\tilde{m}_\Delta = 100$ eV instead, one observes that $T^\tau_{\rm decoh} \gtrsim T_A$ requires $m_\Delta \lesssim 10^7$ GeV. Similarly, in the left panel of Fig. 4 we added as a function of $\tilde{m}_\Delta^{\rm eff}$ the upper bound which holds on m_Δ if one considers this condition rather than the one in Eq. (51). The corresponding region are labeled by "2(3)-flavor" following that we require $T^\tau_{\rm decoh} \gtrsim T_A$ or $T^\mu_{\rm decoh} \gtrsim T_A$. One should close this section by saying again that the use of $T_{\rm decoh}$ as a sharp transition temperature is a reasonable assumption one will make, but it does not probably take into account the fact that partial decoherence could already occur at higher temperature.

3.3 Formal integration of Boltzmann equations

Keeping only leading order terms in Eq. (25), i.e. dropping third and forth terms, an analytic formal integration of the equations responsible for the $B-L$ asymmetry can be accomplished, basically along the same lines of the type-I seesaw case [43]. For definitiveness we will focus on the two flavor regime, results for the three flavor regime can be readily derived following the same procedure we will outline. In the two flavor regime the asymmetry vector introduced in Sec. 3 (see Eq. (28)) is given by

$$\vec{Y}_\Delta = \begin{pmatrix} Y_{\Delta_{\Delta_\alpha}} \\ Y_{\Delta_{B/3-L_a}} \\ Y_{\Delta_{B/3-L_\tau}} \end{pmatrix} \, . \tag{54}$$

In terms of this vector, Eqs. (23) and (25) can be casted in matricial form, namely

$$\frac{d}{dz}\vec{Y}_\Delta(z) = -\left(\frac{Y_{\Sigma_\alpha}}{Y^{\rm Eq}_{\Sigma_\alpha}} - 1\right) D(z)\,\vec{\varepsilon} - D(z)\mathcal{M}(z)\vec{Y}_\Delta(z) \, , \tag{55}$$

with

$$D(z) = \frac{\gamma_{D_\alpha}(z)}{s(z)\,H(z)\,z} \, , \tag{56}$$

and where the *CP-asymmetry-vector* $\vec{\varepsilon}$ is defined as

$$\vec{\varepsilon} = \begin{pmatrix} 0 \\ \epsilon^{\ell_a}_{\Delta_\alpha} \\ \epsilon^{\ell_\tau}_{\Delta_\alpha} \end{pmatrix} \tag{57}$$

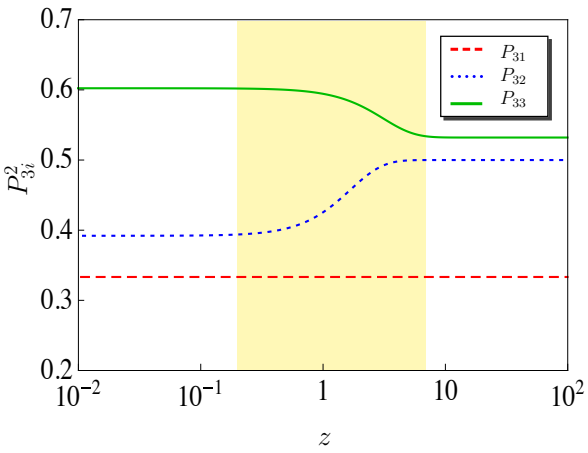

Figure 5: $\mathcal{P}$ *eigenvectors-third-component* $\mathcal{P}_{3i}$ *as a function of* z*. The eigenvectors have been evaluated for the flavor configuration* $B_{\ell_{ii}} = 0$ *and* $B_{\ell_{12}} = B_{\ell_{21}} = (1 - B_\phi)/2$*, with* $B_\phi = 10^{-4}$*. We have checked that this result is quite insensitive to changes in the flavor configuration. The vertical yellow stripe indicates the range where the matrix* $\mathcal{P}$ *slightly depends upon* z*.*

while the *flavor-triplet-coupling-matrix* according to

$$\mathcal{M}(z) = \begin{pmatrix} \frac{1}{Y_\Sigma^{\rm Eq}} - \frac{\sum_i B_{\ell_i} C^\ell_{i\Delta} - B_\phi C^\phi_\Delta}{Y_\ell^{\rm Eq}} & -\frac{\sum_i B_{\ell_i} C^\ell_{ia} - B_\phi C^\phi_a}{Y_\ell^{\rm Eq}} & -\frac{\sum_i B_{\ell_i} C^\ell_{i\tau} - B_\phi C^\phi_\tau}{Y_\ell^{\rm Eq}} \\ -2\sum_j B_{\ell_{aj}} \left(\frac{1}{Y_\Sigma^{\rm Eq}} - \frac{1}{2}\frac{C^\ell_{aj\Delta}}{Y_\ell^{\rm Eq}}\right) & \sum_j B_{\ell_{aj}} \frac{C^\ell_{aja}}{Y_\ell^{\rm Eq}} & \sum_j B_{\ell_{aj}} \frac{C^\ell_{aj\tau}}{Y_\ell^{\rm Eq}} \\ -2\sum_j B_{\ell_{\tau j}} \left(\frac{1}{Y_\Sigma^{\rm Eq}} - \frac{1}{2}\frac{C^\ell_{\tau j\Delta}}{Y_\ell^{\rm Eq}}\right) & \sum_j B_{\ell_{\tau j}} \frac{C^\ell_{\tau ja}}{Y_\ell^{\rm Eq}} & \sum_j B_{\ell_{\tau j}} \frac{C^\ell_{\tau j\tau}}{Y_\ell^{\rm Eq}} \end{pmatrix} . \tag{58}$$

In the case $\mathcal{M}(z) = \mathcal{M}$, the system of equations in (55) can be decoupled via a rotation of the asymmetry vector $\vec{Y}_\Delta$, the matrix accounting for the rotation being determined by the similarity transformation

$$\mathcal{P}^{-1}\,\mathcal{M}\,\mathcal{P} = \hat{\mathcal{M}} \ , \tag{59}$$

which brings $\mathcal{M}$ to diagonal form. Strictly speaking $\mathcal{M}$ does depend on z, but it turns out that the z dependence of the rotation matrix $\mathcal{P}$ is quite moderate. As can be seen in Fig. 5, in the high as well as in the low temperature regime $\mathcal{P}(z) = \mathcal{P}$ whereas within the window $z \subset [0.2, 7]$ there is a dependence, which nevertheless is rather soft.

Thus, taking a z independent change-of-basis-matrix $\mathcal{P}$ and rotating the asymmetry vector as

$$\vec{Y}'_\Delta(z) = \mathcal{P}^{-1}\,\vec{Y}_\Delta \ , \tag{60}$$

we finally get a decoupled system of differential equations:

$$\frac{d}{dz}\vec{Y}'_\Delta(z) = -\left(\frac{Y_{\Sigma_\alpha}}{Y^{\rm Eq}_{\Sigma_\alpha}} - 1\right) D(z)\,\vec{\varepsilon}' - D(z)\hat{\mathcal{M}}(z)\vec{Y}'_\Delta(z) \ , \tag{61}$$

where the *rotated-CP-asymmetry-vector* $\vec{\varepsilon}'$ has been introduced:

$$\vec{\varepsilon}' = \mathcal{P}^{-1}\vec{\varepsilon}\,. \tag{62}$$

The decoupled system of equations in (61) can then be formally integrated through their integrating factor. By doing so, and assuming vanishing primordial asymmetries, $\vec{Y}_\Delta(z_0) = 0$ with $z_0 \ll 1$, the solution reads

$$\vec{Y}'_\Delta(z) = -\int_{z_0}^{z} dz' \, \frac{\gamma_{D_\alpha}(z')}{\gamma_{D_\alpha}(z') + 4\gamma_{A_\alpha}(z')} \frac{dY_{\Sigma_\alpha}(z')}{dz'} \, e^{-\int_{z'}^{z} dz'' D(z'')\hat{\mathcal{M}}(z'')} \, \vec{\varepsilon}' \,. \tag{63}$$

In terms of the "new" asymmetries, and due to the diagonal structure of the matricial damping factor, one can define efficiency functions $\eta'_i(z)$, which account for the evolution of the primed asymmetries and their corresponding values at freeze-out ($z \to \infty$), namely

$$\left[\vec{Y}'_\Delta(z)\right]_i = -\eta'_i(z)\,\varepsilon'_i\, Y^{\rm Eq}_{\Sigma_\alpha}(z_0) \,, \tag{64}$$

where the efficiency functions can be directly read from (63) by taking into account that, as usual, they have been normalized to the scalar triplet equilibrium distribution evaluated at z_0. The evolution of these asymmetries, however, does not describe the evolution of the actual $B/3 - L_i$ asymmetries and instead, as can be seen in (60), a superposition which involves the triplet asymmetry as well. A meaningful description requires switching to the non-primed variables, which yields[7]

$$\vec{Y}_\Delta(z) = -\int_{z_0}^{z} dz' \, \frac{\gamma_{D_\alpha}(z')}{\gamma_{D_\alpha}(z') + 4\gamma_{A_\alpha}(z')} \frac{dY_{\Sigma_\alpha}(z')}{dz'} \, e^{-\int_{z'}^{z} dz'' D(z'')\mathcal{M}(z'')} \, \vec{\varepsilon}\,. \tag{65}$$

In the non-primed basis the matricial damping factor is no longer diagonal and therefore defining efficiency functions, as it was done in the primed basis, is no longer possible: both $B/3 - L_a$ and $B/3 - L_\tau$ are a superposition of two terms weighted by the corresponding CP asymmetries $\epsilon^{\ell_a}_{\Delta_\alpha}$ and $\epsilon^{\ell_\tau}_{\Delta_\alpha}$. Let us discuss this in more detail. The i-th component of the asymmetry vector in (65) can be written as

$$\left[\vec{Y}_\Delta(z)\right]_i = -\int_{z_0}^{z} dz' \, \frac{\gamma_{D_\alpha}(z')}{\gamma_{D_\alpha}(z') + 4\gamma_{A_\alpha}(z')} \frac{dY_{\Sigma_\alpha}(z')}{dz'} \sum_{k=1,2,3} \left[e^{-\int_{z'}^{z} dz'' D(z'')\mathcal{M}(z'')}\right]_{ik} \varepsilon_k \,, \tag{66}$$

thus implying that in the primed basis the flavored asymmetries become

$$\begin{aligned} Y_{B/3-L_a}(z) &= -\left[\eta_{aa}(z)\epsilon^{\ell_a}_{\Delta_\alpha} + \eta_{a\tau}(z)\epsilon^{\ell_\tau}_{\Delta_\alpha}\right] Y^{\rm Eq}_{\Sigma_\alpha}(z_0) \,, \\ Y_{B/3-L_\tau}(z) &= -\left[\eta_{\tau a}(z)\epsilon^{\ell_a}_{\Delta_\alpha} + \eta_{\tau\tau}(z)\epsilon^{\ell_\tau}_{\Delta_\alpha}\right] Y^{\rm Eq}_{\Sigma_\alpha}(z_0) \,, \end{aligned} \tag{67}$$

with the flavored efficiency functions defined as:

$$\eta_{ik}(z) = \frac{1}{Y^{\rm Eq}_{\Sigma_\alpha}(z_0)} \int_{z_0}^{z} dz' \, \frac{\gamma_{D_\alpha}(z')}{\gamma_{D_\alpha}(z') + 4\gamma_{A_\alpha}(z')} \frac{dY_{\Sigma_\alpha}(z')}{dz'} \left[e^{-\int_{z'}^{z} dz'' D(z'')\mathcal{M}(z'')}\right]_{ik} \,. \tag{68}$$

[7]This result has been derived by using $\mathcal{P}e^{\hat{\mathcal{M}}}\mathcal{P}^{-1} = e^{\mathcal{M}}$ and Eq. (24), taking into account that $Y_\Sigma(z)$ follows quite closely the equilibrium distribution function so $y_\Sigma + 1 \simeq 2$.

So, once lepton flavors are taken into account—in general—the efficiencies are no longer flavor diagonal. The presence of the flavor off-diagonal efficiencies is a manifestation of flavor coupling which, in contrast to the type-I seesaw-based leptogenesis case, persists even when $C^{\ell} = \mathbb{I}$, due to the intricate structure of the *flavor-triplet-coupling-matrix*. More precisely this occurs because, in contrast to the type-I seesaw leptogenesis case, an asymmetry in the state generating the $B-L$ asymmetry develops (Y_{Δ_Δ}), and so an additional kinetic equation accounting for this asymmetry turns out to be mandatory. Due to the presence of this equation the asymmetries in flavor a and τ are indirectly coupled, and such coupling becomes manifest in the exponential function in Eq. (68). In other words, unlike standard leptogenesis, flavor coupling effects are unavoidable in scalar triplet leptogenesis.

A specific case where flavored efficiency functions, in the same sense of (64), can be properly defined corresponds to PFL scenarios. What actually happens in those cases is that due to the PFL condition $\sum_i \epsilon^{\ell_i}_{\Delta_\alpha} = 0$, which implies $\epsilon^{\ell}_{\Delta_\alpha} \equiv -\epsilon^{\ell_a}_{\Delta_\alpha} = \epsilon^{\ell_\tau}_{\Delta_\alpha}$, the off-diagonal efficiency functions can be hidden by suitable redefinitions:

$$
\begin{aligned}
Y_{B/3-L_a}(z) &= [\eta_{aa}(z) - \eta_{a\tau}(z)]\, \epsilon^{\ell}_{\Delta_\alpha}\, Y^{\rm Eq}_{\Sigma_\alpha}(z_0) \to \eta_a(z)\, \epsilon^{\ell}_{\Delta_\alpha}\, Y^{\rm Eq}_{\Sigma_\alpha}(z_0)\ , \\
Y_{B/3-L_\tau}(z) &= [\eta_{\tau a}(z) - \eta_{\tau\tau}(z)]\, \epsilon^{\ell}_{\Delta_\alpha}\, Y^{\rm Eq}_{\Sigma_\alpha}(z_0) \to \eta_\tau(z)\, \epsilon^{\ell}_{\Delta_\alpha}\, Y^{\rm Eq}_{\Sigma_\alpha}(z_0)\ ,
\end{aligned}
\tag{69}
$$

and so the total $B-L$ asymmetry can be written as

$$
Y_{\Delta_{B-L}}(z) = [\eta_a(z) + \eta_\tau(z)]\, \epsilon^{\ell}_{\Delta_\alpha}\, Y^{\rm Eq}_{\Sigma_\alpha}(z_0)\ , \tag{70}
$$

with the final value (the value at freeze-out) given by $Y_{\Delta_{B-L}} = Y_{\Delta_{B-L}}(z \to \infty)$.

4 Purely flavored triplet leptogenesis

For concreteness and in order to analyze as well as to demonstrate the viability of this scenario, we will fix the triplet mass spectrum to be hierarchical ($m_{\Delta_\alpha} \ll m_{\Delta_\beta}$ with $\alpha < \beta$) and assume that the $B-L$ asymmetry is entirely due to the dynamics of the lightest state $\Delta_\alpha \equiv \Delta$ (henceforth we drop the triplet generation index). We will also consider two-flavored regime situations where the $B-L$ asymmetry is distributed along the τ and a lepton flavor directions (a being an admixture of μ and e flavors)[8].

As previously argued (see Eq. (20) and the corresponding discussion), when the scalar triplet CP asymmetries arise from the presence of another scalar triplet, there exists an overall regime in which the purely flavored CP asymmetries are larger than the lepton number violating CP asymmetries, thus leading to a natural realization (to a very good approximation) of a PFL successful scenario. Strictly speaking PFL scenarios are defined by the condition $\sum_i \epsilon^{\ell_i} = 0$ [24], however in a more general fashion whenever the condition $|\sum_i \epsilon^{\ell_i}_{\Delta}| < |\epsilon^{\ell_i}_{\Delta}|$ (for any given value of i) is satisfied a PFL scenario can be defined as well.

[8]Note that in the regime where all the charged lepton SM Yukawa interactions are in thermodynamic equilibrium ($T \ll 10^5$ GeV) lepton flavor equilibrating processes would render this PFL scenario unviable [26].

This is actually the condition which is generically satisfied, as soon as Eq. (20) holds, i.e. if one or both scalar triplets couple substantially less to scalars than they do to leptons.

The viability of PFL scenarios demands leptogenesis to take place in the flavored regime, i.e. requires leptogenesis to occur at $T \leq T_{\rm decoh}$ (see Sec. 3.2), and furthermore it requires more than a dominance of the purely flavored CP asymmetries. Since the sum of the purely flavored CP asymmetries vanishes (total lepton number is conserved), if there were only source terms, a net non-vanishing $B-L$ asymmetry would not develop due to an exact cancellation among the different $B/3-L_i$ asymmetries. This cancellation has to be mandatorily avoided in order that a net non-vanishing total $B-L$ asymmetry develops. In type-I seesaw, this is possible due to the lepton flavor dependence of the washout effect, which allows the $B/3-L_i$ asymmetries to be washed-out in different amounts. In other words, the production of a net $B-L$ asymmetry in the PFL type-I case, which involves L-conserving CP asymmetries as well, is closely related to the action of L-violating inverse decay rates larger than the Hubble Universe expansion rate (fast L-violating inverse decays), so that they reprocess the $B/3-L_i$ asymmetries in different amounts, in such a way that these asymmetries do not compensate each other anymore.

In the type-II scenario a similar effect is also possible, provided decay/inverse decay to leptons and to scalars reach thermal equilibrium at some stage during the production of the $B-L$ asymmetry, so that L-violating processes do induce a washout. Additionally, and this is a new effect which does not exist in the PFL type-I scenario, this is also possible even if the L-breaking processes present in the heat bath never reach thermal equilibrium.

Let us explain already at this point how does this new effect work. To this end we display in Fig. 6 the evolution of the different abundances as a function of z for the following parameter choice[9]: $\epsilon^{\ell}_{\Delta} \equiv \epsilon^{\ell_\tau}_{\Delta} = -\epsilon^{\ell_a}_{\Delta} = 1$, $m_{\Delta} = 10^9$ GeV, $\tilde{m}_{\Delta} = 10^{-2}$ eV, $B_{\phi} = 10^{-4}$, $B_{\ell_{aa}} = B_{\ell_{a\tau}} = 0$ and $B_{\ell_{\tau\tau}} = 1 - B_{\phi}$. As we will discuss further on in this section, this $B_{\ell_{ij}}$ flavor configuration maximizes the efficiency.

Fig. 3 (left-hand side plot) clearly shows that for $B_{\phi} = 10^{-4}$ the inverse decays $\phi\phi \to \Delta$ have always a rate slower than the Hubble expansion rate. The fact that for the type-II PFL case, we do get nevertheless a net non-vanishing $B-L$ asymmetry can then at first sight appear to be counterintuitive. If for instance only the channel to leptons does get in thermal equilibrium, as it turns out to be the case for $B_{\phi} = 10^{-4}$, the scalar triplets have effectively lepton number $L = -2$ and the only active (fast) inverse decays in the thermal bath, $\Delta \to \bar{\ell}\bar{\ell}$ and $\bar{\Delta} \to \ell\ell$, do not break total lepton number.

However, although the scalar doublet channel never reaches thermal equilibrium, still a portion of the scalar triplets in the heat bath undergoes decays to scalar doublets ($\Delta \to \phi\phi$), and these processes do break L. If the processes $\Delta \to \phi\phi$ and $\bar{\Delta} \to \bar{\phi}\bar{\phi}$ take place at different rates, the thermal bath gets a fraction of total lepton number each time these reactions occur. Quantitatively this means that we can define an effective $B-L$ yield, $Y^{\rm eff}_{\Delta_{B-L}}$, determined by the counting of how many scalar triplets decay times their

[9]Using Eq. (49), this choice corresponds to $\tilde{m}^{\rm eff}_{\Delta} = 1$ eV. From Fig. 4, it is clear that this parameter choice ensures the $B-L$ asymmetry generation process to take place in the two-flavor regime where Eq. (43) holds.

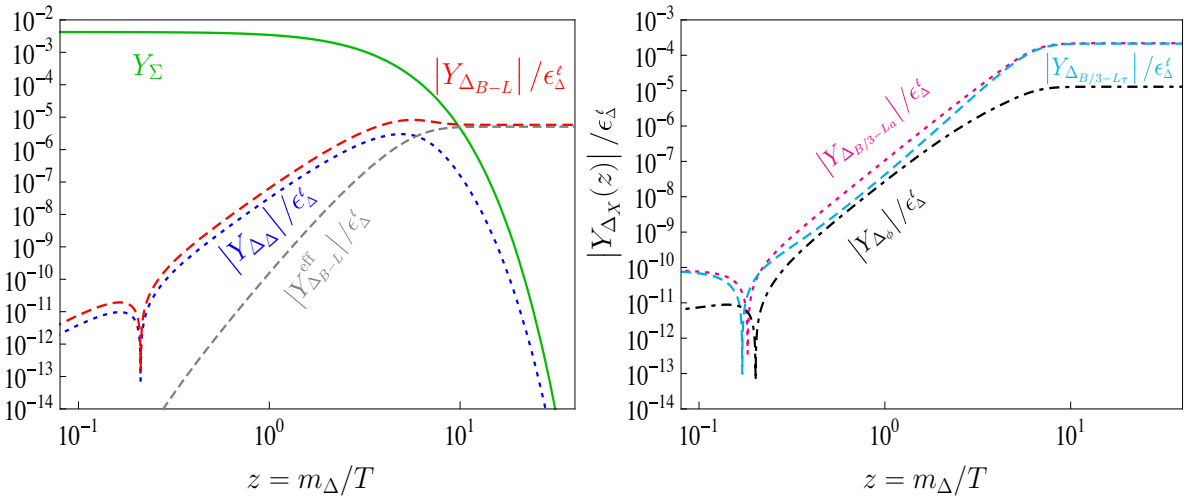

Figure 6: *Evolution of the different asymmetries* Y_Σ, Y_{Δ_Δ}, $Y_{\Delta_{B-L}}$, Y_{Δ_ϕ} *and* $Y^{eff}_{\Delta_{B-L}}$ *as given by Eq. (71), as a function of* z *for the flavor configuration:* $B_{\ell_{aa}} = B_{\ell_{a\tau}} = 0$, $B_{\ell_{\tau\tau}} = (1 - B_\phi)$. *The remaining parameters have been fixed according to:* $m_\Delta = 10^9$ *GeV,* $\tilde{m}_{\Delta_\alpha} = 10^{-2}$ *eV and* $B_\phi = 10^{-4}$.

branching ratio into scalar doublets, namely

$$Y^{\rm eff}_{\Delta_{B-L}}(z) \approx -2 \int_{z_0}^{z} \frac{dz'}{sHz'} \frac{Y_{\Delta_\Delta}}{Y^{\rm Eq}_\Sigma} B_\phi \gamma_D \ , \tag{71}$$

where the factor 2 comes from the fact that the decay to scalar doublets violates lepton number by 2 units. This effective quantity holds for the total $B - L$ asymmetry available if one assigns to Δ ($\bar{\Delta}$) a lepton number equal to -2 (2), as we have previously pointed out. It is related to the usual $B - L$ yield (where triplets have vanishing lepton number) according to

$$Y_{\Delta_{B-L}}(z) = -2Y_{\Delta_\Delta}(z) + Y^{\rm eff}_{\Delta_{B-L}}(z) \, . \tag{72}$$

Since ultimately all triplets decay (their density vanishes), the final $B - L$ asymmetry simply reads

$$Y_{\Delta_{B-L}} = Y^{\rm eff}_{\Delta_{B-L}}(z \to \infty) \approx -2 \int_{z_0}^{\infty} \frac{dz'}{sHz'} \frac{Y_{\Delta_\Delta}}{Y^{\rm Eq}_\Sigma} B_\phi \gamma_D \ . \tag{73}$$

In order to prove that this formula reproduces the correct $B-L$ asymmetry yield at freeze-out, we have inserted in Eq. (71) the Y_{Δ_Δ} asymmetry obtained by solving numerically the set of Boltzmann equations. The result is shown in Fig. 6 (left-hand side plot) by the dashed gray curve. It clearly shows that Eq. (73) reproduces very well the numerical result (red dashed curve) for the $B - L$ asymmetry yield at freeze-out, up to a small deviation of order 30%. This deviation can be fully traced back to the effect of the inverse decay processes, $\phi\phi \to \Delta$ and $\bar{\phi}\bar{\phi} \to \bar{\Delta}$, i.e. of the term $\propto B^\alpha_\phi$ in Eq. (23). These scalar inverse decays are not as numerous as scalar decays but not negligible either.

The generation of a baryon asymmetry, through decays rather than through inverse decay washout effects, is thus closely related to the possibility of creating a scalar triplet asymmetry (something obviously not possible for a right-handed neutrino due to its Majorana nature). The role of flavor effects is in fact to generate such a triplet asymmetry. To see that, it is useful to write down the relevant terms in Eq. (23),

$$\dot{Y}_{\Delta_\Delta} \supset \sum_k \sum_i B_{\ell_i} C^\ell_{ik} \frac{Y_{\Delta_k}}{Y^{\rm Eq}_\ell} \gamma_D \ . \tag{74}$$

This expression clearly shows that a triplet asymmetry can be generated by two kinds of flavor effects:

- The first possibility arises if the C^ℓ_{ij} have a flavor structure. For instance, if the τ Yukawa is in equilibrium, once a lepton doublet ℓ_τ is produced, it has the time to interact through the Yukawa coupling and a fraction of the τ flavor is transferred from ℓ_τ lepton doublets to e_τ lepton singlets, while this is not the case for flavor a. These transferred fractions are just given by the C^ℓ matrices which are dictated by the chemical potential equilibrium equations, see Eq. (26). This means that there are less ℓ_τ than ℓ_a lepton doublets available for inverse decays to scalar triplets. So, even if there is no flavor structure in the branching ratios (i.e. $B_{\ell_a} = B_{\ell_\tau}$) and even if, at the onset, $Y_{\Delta_{L_\tau}} = -Y_{\Delta_{L_a}}$, the number of Δ produced is different from the number of $\bar{\Delta}$ produced because their production rate is proportional to $Y_{\bar{\ell}_\tau} + Y_{\bar{\ell}_a}$ and $Y_{\ell_\tau} + Y_{\ell_a}$ respectively, which are unequal[10].

- The second possibility arises from the flavor structure of scalar triplet decays, i.e. the B_{ℓ_i}. If $B_{\ell_a} \neq B_{\ell_\tau}$, a triplet asymmetry can be produced even if the C^ℓ coefficients do not distinguish the a and τ flavors. In this case, even if at the onset, $Y_{\Delta_{L_\tau}} = -Y_{\Delta_{L_a}}$, with for example $B_\tau \gg B_a$ and $Y_{L_\tau} > 0$, inverse decays involving the τ flavor are much more frequent than those involving the a flavor and inverse decays $\ell_\tau \ell_{a,\tau} \to \bar{\Delta}$ occur more frequently than $\ell_a \ell_{a,\tau} \to \bar{\Delta}$ inverse decays, resulting in the generation of a Y_{Δ_Δ} asymmetry (of negative sign in this case).

In other words, in the PFL case there is no L-violating CP asymmetry. The fact that a final $B-L$ asymmetry can be generated in this case, even without L-violating processes attaining thermal equilibrium, i.e. $B_\phi \ll B_\ell$, can be understood as a three step process, summarized in Fig. 7. Firstly, an asymmetry $Y_{\Delta_{L_\tau}} = |Y_{\Delta_{L_a}}| \neq 0$ is created from the source term in Eq. (25). Secondly, thanks to flavor effects, this asymmetry induces a triplet asymmetry via Eq. (74), due to the flavor structure encoded in C^ℓ_{ij} and/or due to the flavor structure encoded in the B_{ℓ_i}. And finally, once a scalar triplet asymmetry is created, a $B-L$ asymmetry develops in turn because each time a triplet (anti-triplet) decays to scalars, a pair less of anti-leptons (leptons) is produced back from the decay of

[10]It is worth noting that we have the same reprocessing concerning the ϕ asymmetry created from the slow Δ decays. This latter asymmetry is partly reprocessed through L-conserving SM Yukawa interactions into chiral asymmetries for charged leptons, which modifies back the Δ asymmetry, hence the number of Δ decaying into SM scalars, hence the $B-L$ asymmetry. This effect is nevertheless mild.

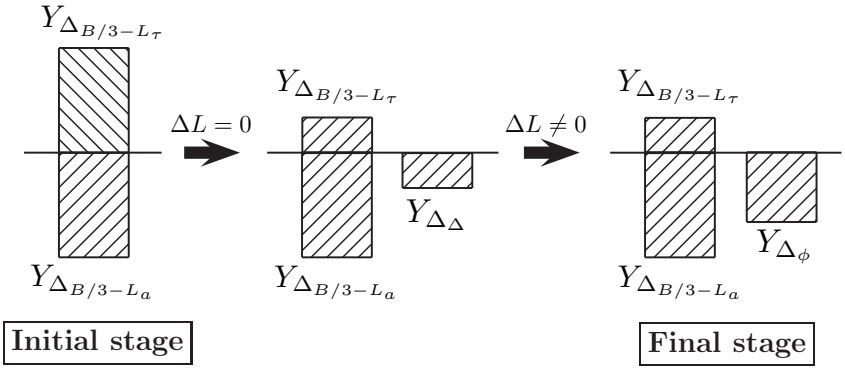

Figure 7: *Sketch of the type-II PFL mechanism. See text for further details.*

a triplet (anti-triplet). The more Y_{Δ_Δ} asymmetry is produced, the bigger the efficiency. This PFL production mechanism, based on the chain of processes $\ell_i\ell_j \leftrightarrow \bar{\Delta} \to \bar{\phi}\bar{\phi}$ and $\bar{\ell}_i\bar{\ell}_j \leftrightarrow \Delta \to \phi\phi$, is therefore very different from the PFL type-I scenario. It stems from the fact that in the type-II scenario, a seesaw state asymmetry develops, and in its last step this asymmetry generates a final $B-L$ asymmetry from a production mechanism which is due to out-of-thermal equilibrium decays, i.e. from the $\Delta \to \phi\phi$ and $\bar{\Delta} \to \bar{\phi}\bar{\phi}$ L-violating processes ($B_\phi \ll B_\ell$)[11].

Let us emphasize once again that this $B_\phi \ll 1$ case is the situation which leads naturally to PFL, since this condition leads to a natural dominance of the purely flavored CP asymmetries. It must be noted that PFL could nevertheless work for larger values of B_ϕ too, in a way more similar to the more involved PFL scenarios in the type-I context, see Sec. 4.1.3 below.

In the following section we will analyze, along these lines, the efficiency dependence upon the relevant parameters. We will discuss in particular the flavor configurations which minimize, or maximize, the production of Y_{Δ_Δ}. We will then discuss the flavored CP asymmetry parameter dependence and show how the configurations that maximize the efficiency minimize the flavored CP asymmetry. The production of the $B-L$ asymmetry, which is given by the product of the flavored CP asymmetry and the efficiency, results therefore from the balance of both effects.

4.1 PFL scenario efficiency

The problem of quantifying the efficiency is—in principle—an eight parameters problem: $\epsilon_\Delta^{\ell_\tau,a}$, m_Δ, $\tilde{m}_\Delta$, B_ϕ, $B_{\ell_{aa}}$, $B_{\ell_{\tau\tau}}$ and $B_{\ell_{a\tau}}$, which reduces to six parameters due to the

[11]This production mechanism driven by a tiny coupling is in many ways similar to the dark matter freeze-in production mechanism, as Eq. (73) shows. However there are important differences. Firstly, this equation involves as a source term an asymmetry, Y_{Δ_Δ}, and not the symmetric component of a particle species as in the freeze-in scenario. Secondly, since we are dealing with decay rates much larger that the one of the dark matter freeze-in, still a small amount of inverse decays occurs, as we have pointed out.

constraints $B_\ell + B_\phi = 1$ and $\epsilon^\ell_\Delta \equiv \epsilon^{\ell_\tau}_\Delta = -\epsilon^{\ell_a}_\Delta$. Since the efficiency does not depend on ϵ^ℓ_Δ—see Eq. (70)—we will analyze the dependence of the efficiency upon the 5 remaining parameters: m_Δ, $\tilde{m}_\Delta$, B_ϕ, $B_{\ell_{aa}}$ and $B_{\ell_{\tau\tau}}$.

We start by analyzing the dependence upon $B_{\ell_{ij}}$ for fixed B_ϕ, m_Δ and $\tilde{m}_\Delta$. We will see that different flavor configurations ($B_{\ell_{ij}}$ configurations) will produce a minimal or maximal efficiency. However, as we will latter show in Sec. 4.2, the configurations that maximize the efficiency do not necessarily maximize the final $B-L$ asymmetry. We then proceed by analyzing the dependence of the efficiency with $\tilde{m}_\Delta$ for fixed B_ϕ, m_Δ and $B_{\ell_{ij}}$, and finally the dependence of the efficiency with B_ϕ for fixed $\tilde{m}_\Delta$, m_Δ and $B_{\ell_{ij}}$. This will allow us to understand and distinguish the main features of the type-II seesaw PFL scenario.

4.1.1 Efficiency: $B_{\ell_{ij}}$ dependence

In order to proceed, we first solve numerically the system of kinetic equations in (23)-(25) for different flavor configurations. We then provide some physical arguments supporting the special flavor configurations that maximize/minimize the efficiency. For concreteness, we fix three out of the five relevant parameters as follows:

$$m_\Delta = 10^9\,\text{GeV}\ , \quad \tilde{m}_\Delta = 10^{-2}\,\text{eV}\ , \quad B_\phi = 10^{-4}\ . \tag{75}$$

Once these parameters are fixed, the efficiency is entirely dictated by the flavor configurations determined by the values of the $B_{\ell_{ij}}$ parameters. It turns out that the flavor dependence is well described by the quantity:

$$R \equiv \frac{B_{\ell_a}}{B_{\ell_\tau}} = \frac{B_{\ell_{aa}} + B_{\ell_{a\tau}}}{B_{\ell_{\tau a}} + B_{\ell_{\tau\tau}}}\ , \tag{76}$$

which represents the ratio of triplet decay branching ratios to different lepton-flavor final states. The importance of this quantity can be understood from Eq. (74), where we see that it is precisely through the B_{ℓ_i} that a triplet asymmetry is generated. We plot in Fig. 8 the efficiency as a function of this parameter R for the parameters fixed according to Eq. (75).

A viable scalar triplet leptogenesis setup requires—of course—consistency with neutrino data [1, 3, 2]. If the most relevant contribution to the neutrino mass matrix in Eq. (6) is given by the lightest triplet, which can be regarded as a quite reasonable possibility (assumption), the determination of the available flavor configurations can be done directly via neutrino oscillation data. We present in Fig. 9 the constraints on R (left panel) and on the ratios of branching ratios $B_{\ell_{ii}}/B_{\ell_{ij}}$ (right panel) as a function of the lightest neutrino mass, for the normal (green) and inverted (red) light neutrino mass spectrum. We fixed the neutrino oscillation parameters according to their upper and lower 3σ limits [1]. It can be seen that the R configuration leading to a vanishing $B-L$ asymmetry, although showing up at the 3σ level in the normal spectrum case, can be readily evaded, thus showing the viability of the PFL scenario even in its most constrained form.

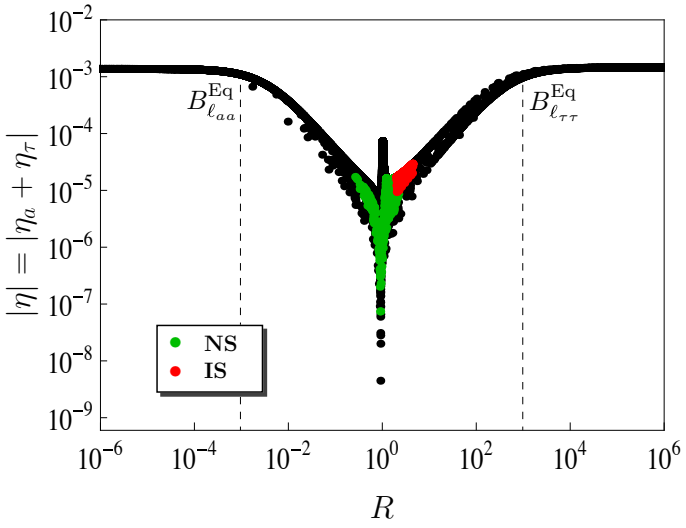

Figure 8: *Efficiency as a function of the R parameter for* $m_\Delta = 10^9$ *GeV,* $\tilde{m}_\Delta = 10^{-2}$ *eV and* $B_\phi = 10^{-4}$. *The green (red) dots indicate the allowed range for the efficiency, as required by neutrino data (*3σ *level [1]) for the inverted (normal) hierarchical light neutrino mass spectrum. In addition to the constraints on R, we also took into account the constraints imposed by data on the different* $B_{\ell_{ij}}$ *elements (see Fig. 9). We stress that these constraints apply only if the neutrino mass matrix is entirely dominated by the lightest scalar triplet contribution.*

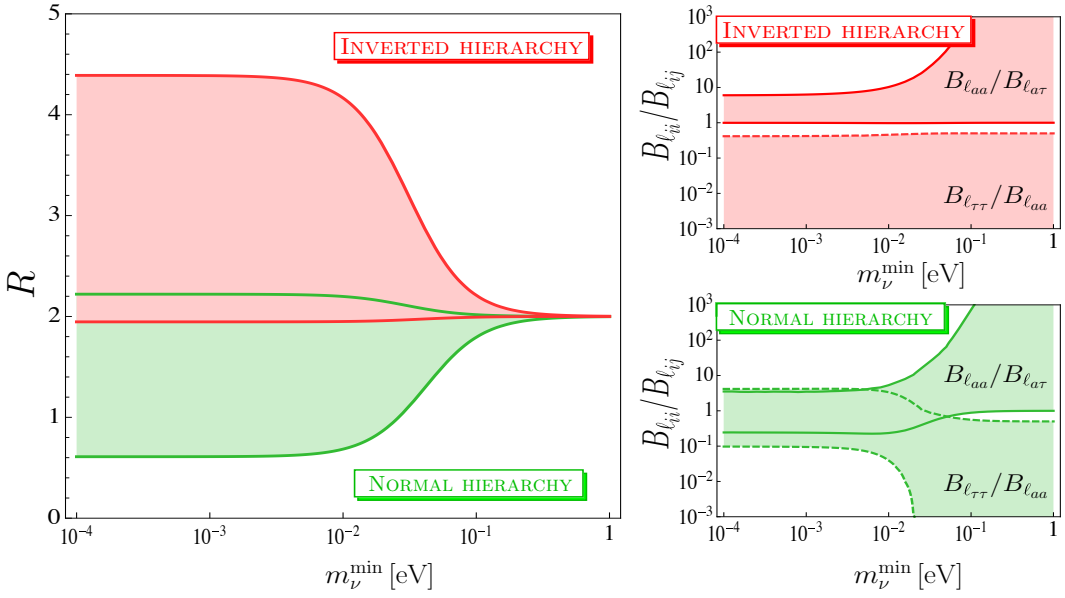

Figure 9: *Allowed ranges for R (left plot) and the ratios of branching ratios* $B_{\ell_{ii}}/B_{\ell_{ij}}$ *(right plots) as a function of the lightest neutrino mass for both normal (green) and inverted mass spectrum (red). The results have been derived by varying the neutrino oscillation parameters in the* 3σ *range according to [1].*

Fig. 8 clearly shows that the efficiency exhibits four special configurations, namely (*i*, *ii*) two global maxima at $R \ll 1$ and $R \gg 1$, (*iii*) one local maximum and (*iv*) one global minimum near $R \sim 1$. We now aim to understand the physical reasons behind these special configurations.

Configurations (*i*) and (*ii*): following Eq. (76), these global maxima correspond to the flavor alignments $B_{\ell_a} \ll B_{\ell_\tau}$ and $B_{\ell_a} \gg B_{\ell_\tau}$. The effect seems entirely driven by the B_{ℓ_i}, so we will not consider the possible effects of the C^ℓ_{ij} and C^ϕ_k elements in the analysis. More precisely, these maxima are reached whenever the inverse decays involving the a or τ flavor never enter in thermal equilibrium, i.e. for $B_{\ell_{ii}} < B^{\rm Eq}_{\ell_{ii}}$ where $B^{\rm Eq}_{\ell_{ii}}$ is determined by:

$$B^{\rm Eq}_{\ell_{ii}} \, \frac{Y^{\rm Eq}_\Sigma}{Y^{\rm Eq}_\ell} \, \frac{\gamma_D}{H n_\gamma}\Big|_{\rm max} = 1 \quad \text{which gives} \quad B^{\rm Eq}_{\ell_{ii}} \approx 10^{-3} \, , \tag{77}$$

where we used in the last equality the parameter values given in Eq. (75). This value is in good agreement with the numerical results shown in Fig. 8, where the two maxima are reached for $R \lesssim 10^{-3}$ and $R \gtrsim 10^3$. For these configurations, only the asymmetry produced in one flavor is transferred through inverse decays $\ell_i \ell_i \to \bar{\Delta}$ to a triplet asymmetry, which is therefore maximal since the two flavor asymmetries have opposite signs. As a consequence, one asymmetry is depleted through the chain $\ell_i \ell_i \leftrightarrow \bar{\Delta} \to \bar{\phi}\bar{\phi}$, while the other flavor asymmetry remains unaffected, clearly leading to a maximal efficiency.

Configuration (*iii*): this local maximum is in fact reached for $R \approx 1$ when $B_{\ell_{ii}} \ll B_{\ell_{a\tau}}$. In this configuration, only the inverse decays $\ell_a \ell_\tau \to \bar{\Delta}$ reach thermal equilibrium, and one expects no production of a triplet asymmetry, and therefore no production of a final $B - L$ asymmetry, since the flavor asymmetries are depleted by the same amount. However, this is not the case because the C^ℓ_{ij} elements have a flavor structure, which plays a crucial role. The point is that when inverse decays are in thermal equilibrium, the combination of processes $\ell_a \ell_\tau \leftrightarrow \bar{\Delta} \to \bar{\phi}\bar{\phi}$ and $\bar{\ell}_a \bar{\ell}_\tau \leftrightarrow \Delta \to \phi\phi$ tends to equilibrate the flavor asymmetries in lepton doublets $Y_{\Delta_{\ell_\tau}} \approx -Y_{\Delta_{\ell_a}}$, while in the meantime decreasing the separated asymmetries by a small amount[12]. But due to the chemical equilibrium conditions, the total lepton flavors asymmetries $Y_{\Delta_{B/3-L_i}}$ are in general different. Indeed, using Eq. (27), the total $B - L$ asymmetry at freeze-out is related to the lepton flavor doublet asymmetries through:

$$Y_{\Delta_{B-L}} = Y_{\Delta_a} + Y_{\Delta_\tau} = -\frac{Y_{\Delta_{\ell_a}} \left(C^\ell_{\tau\tau} - C^\ell_{\tau a}\right) + Y_{\Delta_{\ell_\tau}} \left(C^\ell_{aa} - C^\ell_{a\tau}\right)}{C^\ell_{\tau\tau} C^\ell_{aa} - C^\ell_{a\tau} C^\ell_{\tau a}} \, . \tag{78}$$

In the PFL regime, in the case where the final lepton doublet asymmetries are equal and opposite, $Y_{\Delta_{\ell_\tau}} \approx -Y_{\Delta_{\ell_a}}$ (as for the case $B_{\ell_{ii}} = 0$), a final $B - L$ asymmetry can be produced only if the C^ℓ_{ij} elements have a flavor structure. This $B - L$ asymmetry can be quite large because the flavor asymmetries in lepton doublets $Y_{\Delta_{\ell_i}}$ decrease only slightly for this special configuration.

[12]Indeed, if $Y_{\ell_a} \cdot Y_{\ell_\tau} > Y_{\bar{\ell}_a} \cdot Y_{\bar{\ell}_\tau}$, that is if $Y_{\Delta_{\ell_\tau}} + Y_{\Delta_{\ell_a}} > 0$, there will be more $\ell_a \ell_\tau \leftrightarrow \bar{\Delta} \to \bar{\phi}\bar{\phi}$ processes than $\bar{\ell}_a \bar{\ell}_\tau \leftrightarrow \Delta \to \phi\phi$ processes, so that statistically $Y_{\Delta_{\ell_\tau}} + Y_{\Delta_{\ell_a}}$ will decrease, as well as the separated asymmetries $Y_{\Delta_{\ell_\tau}}$ and $|Y_{\Delta_{\ell_a}}|$. This lasts until $Y_{\Delta_{\ell_\tau}} \approx -Y_{\Delta_{\ell_a}}$, and from that moment no more triplet asymmetry can be generated and the asymmetries $Y_{\Delta_{\ell_\tau}}$ and $|Y_{\Delta_{\ell_a}}|$ are left invariant.

Any significant deviation from this special configuration, e.g. $B_{\ell_{ii}} > B^{\rm Eq}_{\ell_{ii}}$, would not only tend to equilibrate the flavor asymmetries in the lepton doublets, but also the $Y_{\Delta_{\ell_i}}$ separately through the chain $\bar{\ell}_i\bar{\ell}_i \leftrightarrow \Delta \to \phi\phi$. All in all, the efficiency has in consequence a local maximum for $B_{\ell_{a\tau}} \approx (1 - B_\phi)/2$.

Configuration (*iv*): shifted to the left of the maximum defining configuration (*iii*), a minimal efficiency (almost vanishing efficiency) can be seen, it lies at about $R \approx 3/4$. In order to understand the reason for this configuration to show up, we can look in a first step if analytically the efficiency may vanish for some value of the flavor parameters $B_{\ell_{ij}}$. Using Eq. (70), we see that a vanishing efficiency is obtained whenever $\eta_\tau(z) = -\eta_a(z)$ for all z, which means through Eq. (68):

$$\sum_{i,k=2,3} \left(e^{-\int_{z_0}^{z} dz' D(z') \mathcal{M}(z')} \right)_{ik} (-1)^{1+k} = 0 \quad \forall z \ , \tag{79}$$

which is satisfied as long as all the coefficients of the exponential power series expansion vanish, i.e.

$$\sum_{i,k=2,3} \int_{z_0}^{z} dz' D(z') (-1)^{1+k} \left[\mathcal{M}_{ik}(z') - \frac{1}{2} \int_{z_0}^{z} dz'' D(z'') \sum_{j=1}^{3} \mathcal{M}_{ij}(z') \mathcal{M}_{jk}(z'') + \dots \right] = 0 \ . \tag{80}$$

We have found this turns out to be the case if the *flavor-triplet-coupling-matrix* entries satisfy the following two conditions

$$\mathcal{M}_{12} = \mathcal{M}_{13} \quad \text{and} \quad \sum_{i,k=2,3} (-1)^{1+k} \mathcal{M}_{ik} = 0 \ , \tag{81}$$

where the corresponding elements must not depend on z, which is indeed our case—see Eq. (58). This result in turn can be understood using Eqs. (23) and (25). In the two flavor PFL scenario, since the source terms for both flavors are equal and opposite, a vanishing efficiency will be generated if the washouts of the two flavors are also equal and opposite, which is nothing but the conditions in Eq. (81).

More precisely, for this to be achieved, we need that $Y_{\Delta_\tau} = -Y_{\Delta_a}$ remains valid at any time. As Eq. (25) shows, this requires: (a) $Y_{\Delta_\Delta} = 0$ and (b) $\sum_{i,j,k} C^{\ell}_{ijk} B_{\ell_{ij}} Y_{\Delta_k} = 0$ at any time. These two relations hold simultaneously if both conditions in Eq. (81) are fulfilled. Indeed, if relation (a) holds, (b) can be rewritten as the second condition in Eq. (81). On the other hand, if relation (b) holds, (a) can be rewritten using Eq. (25) as $\sum_{i,k} (C^{\ell}_{ik} B_{\ell_i} - B_\phi C^{\phi}_{k}) Y_{\Delta_k} = 0$, which is nothing but the first condition in Eq. (81).

Using Eq. (58), these conditions can be simultaneously fulfilled only in the limit $B_\phi \to 0$, in which case the triplet flavor configuration must satisfy the simple relation:

$$R = \frac{B_{\ell_{aa}} + B_{\ell_{a\tau}}}{B_{\ell_{\tau a}} + B_{\ell_{\tau\tau}}} = \frac{C^{\ell}_{\tau\tau} - C^{\ell}_{\tau a}}{C^{\ell}_{aa} - C^{\ell}_{a\tau}} \approx 0.74 \ . \tag{82}$$

Strictly speaking, since $B_\phi \neq 0$, the efficiency is not vanishing for any value of $B_{\ell_{ij}}$. However, for small B_ϕ, the efficiency does not vanish exactly anymore but shows now a minimum for $R \approx 3/4$, which is in good agreement with the numerical results shown in Fig. 8.

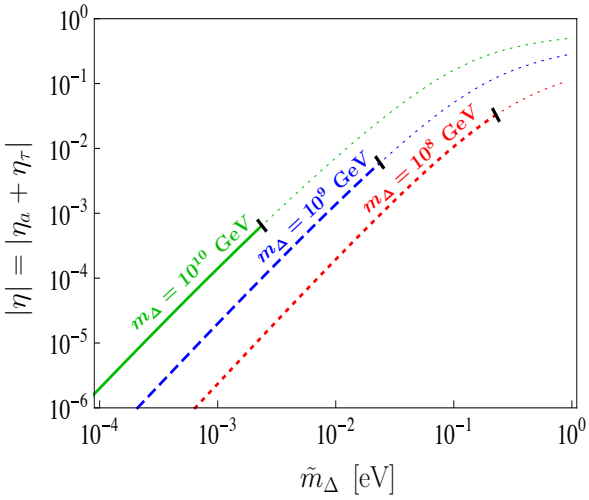

Figure 10: *Efficiency as a function of $\tilde{m}_\Delta$ for several values of the scalar triplet mass. The parameters have been fixed according to $B_\phi = 10^{-4}$ and $B_{\ell_{aa}} = B_{\ell_{a\tau}} = 0$. The lines are cut whenever the 2-flavor regime condition ceases to be fulfilled (see Sec. 3.2).*

4.1.2 Efficiency: $\tilde{m}_\Delta$ dependence

By fixing $B_\phi = 10^{-4}$ as in the previous section, and taking as an example $B_{\ell_{aa}} = B_{\ell_{a\tau}} = 0$, and $B_{\ell_{\tau\tau}} = 1 - B_\phi$, we display in Fig. 10 the dependence of the efficiency with $\tilde{m}_\Delta$, for the three benchmark triplet masses $m_\Delta = 10^8, 10^9, 10^{10}$ GeV. It can be seen that irrespective of the triplet mass, the smaller $\tilde{m}_\Delta$ the smaller the resulting efficiency. The reason for this behavior follows directly from the relative strength of gauge and Yukawa induced reactions: the larger $\tilde{m}_\Delta$ the most likely triplets will decay rather than scatter, thus implying a larger efficiency.

On the other hand, we see that the efficiency decreases with m_Δ. This is also due to gauge reactions: the smaller m_Δ the most likely the triplet will scatter rather than decay, thus implying a smaller efficiency. More precisely, as for the unflavored case, when gauge scatterings are faster than decays they suppress $Y_\Sigma - Y_\Sigma^{Eq}$ in Eq. (24) by a factor γ_D/γ_A, which implies an equal suppression of the source term in Eq. (25).

In the unflavored case one can distinguish two regimes [15], the gauge and Yukawa regimes, depending on the values of m_Δ and $\tilde{m}_\Delta$. While in the unflavored case a maximum efficiency is obtained at the transition between both regimes, this is in general not anymore the case in the flavored leptogenesis scenario. Depending on the flavor configuration, a maximum efficiency can be obtained far in the Yukawa regime because of flavor effects, see Sec. 5 for a more detailed explanation.

4.1.3 Efficiency: B_ϕ dependence

We present in Fig. 11 the dependence of the efficiency upon B_ϕ in the range $[10^{-6}, 1]$ for fixed values of m_Δ and $\tilde{m}_\Delta$. We considered two particular flavor configurations for $B_{\ell_{ij}}$. The red curve (configurations (a)) corresponds to one of the two flavor configurations that

maximize the efficiency (see Sec. 4.1.1). The blue curve (configurations (b)) corresponds instead to the configuration $B_{\ell_{aa}} = B_{\ell_{\tau\tau}}/99 = (1 - B_\phi)/100$ and $B_{\ell_{a\tau}} = 0$. These two configurations show two different behaviors, that are in fact representative of any other flavor configuration.

For $B_\phi \leq 10^{-1}$, which is the interesting region for this PFL scenario, we can distinguish two distinct regimes. They are separated by $B_\phi^{\rm Eq}$, the value at which the inverse decays $\phi\phi \to \Delta$ become active, determined by the condition

$$B_\phi^{\rm Eq} \, \frac{Y_\Sigma^{\rm Eq}}{Y_\ell^{\rm Eq}} \, \frac{\gamma_D}{H n_\gamma}\Big|_{\rm max} = 1 \quad \text{which gives} \quad B_\phi^{\rm Eq} \approx 10^{-3} \, , \tag{83}$$

where we used in the last equality the parameter value domain-of-validity $\tilde{m}_\Delta = 10^{-2}$ eV. The way the efficiency scales with B_ϕ depends on the flavor configurations. For $B_\phi \lesssim B_\phi^{\rm Eq}$ the efficiency always increases with B_ϕ as a result of the fact that the larger B_ϕ the faster the decay to SM scalars, as can be seen in Eq. (73), but the exact scaling actually also depends on the interplay of the Y_{Δ_Δ} and $Y_{\Delta_{B/3-L_i}}$ asymmetries.

Now, as soon as $B_\phi \gtrsim B_\phi^{\rm Eq}$, inverse decays $\phi\phi \to \Delta$ become efficient, implying that lepton number is broken by processes in thermal equilibrium (fast processes). This brings a new $\sqrt{B_\phi}$ suppression in the efficiency, resulting in an efficiency increasing less with B_ϕ or even decreasing, depending on the flavor configuration, see Fig. 11.

To conclude, we see that for the flavor configuration that maximizes the efficiency, the value of B_ϕ which gives the maximal efficiency is obtained for $B_\phi \sim B_\phi^{\rm Eq}$, that is to say for the value of B_ϕ at which the $\phi\phi \to \Delta$ inverse decays are about to be active. In this case, the efficiency can be as large as unity for values of $m_\Delta \gtrsim 10^{12}$ GeV, or less for smaller values of m_Δ (due to the gauge scattering thermalization effect). For other configurations that lead to smaller efficiencies, the maximum efficiency is obtained for much larger values of $B_\phi \sim 1$.

4.2 Minimal and maximal $B - L$ asymmetry

As stressed above, a PFL scenario is naturally favored as soon as $\epsilon_{\Delta_\alpha}^{\ell_i(\not{F})}$ dominates the CP asymmetry, which naturally holds if Yukawa couplings are larger than scalar couplings, i.e. when Eq. (20) holds. This equation can also be recasted in terms of the triplet branching ratios to scalar and lepton final states

$$\sqrt{\frac{B_\phi^\alpha B_\phi^\beta}{B_\ell^\alpha B_\ell^\beta}} \ll \frac{m_{\Delta_\alpha}}{m_{\Delta_\beta}} \frac{{\rm Tr}[\mathcal{M}_\alpha^\nu \mathcal{M}_\beta^{\nu\dagger}]}{\tilde{m}_{\Delta_\alpha} \tilde{m}_{\Delta_\beta}} \leq \frac{m_{\Delta_\alpha}}{m_{\Delta_\beta}} \, , \tag{84}$$

where the last inequality comes from the Cauchy-Schwarz inequality:

$$|{\rm Tr}\,[AB]| \leq \sqrt{{\rm Tr}\,[AA^\dagger]} \sqrt{{\rm Tr}\,[BB^\dagger]} \, . \tag{85}$$

As an example, taking a smooth triplet mass hierarchy $m_{\Delta_\alpha}/m_{\Delta_\beta} \sim 10^{-1}$ (10^{-2}) and assuming the upper bound ${\rm Tr}[\mathcal{M}_\alpha^\nu \mathcal{M}_\beta^{\nu\dagger}] \approx \tilde{m}_{\Delta_\alpha} \tilde{m}_{\Delta_\beta}$, a PFL scenario will be naturally dominant as soon as $B_\phi^{\alpha,\beta} \ll 10^{-1}$ (10^{-2}).

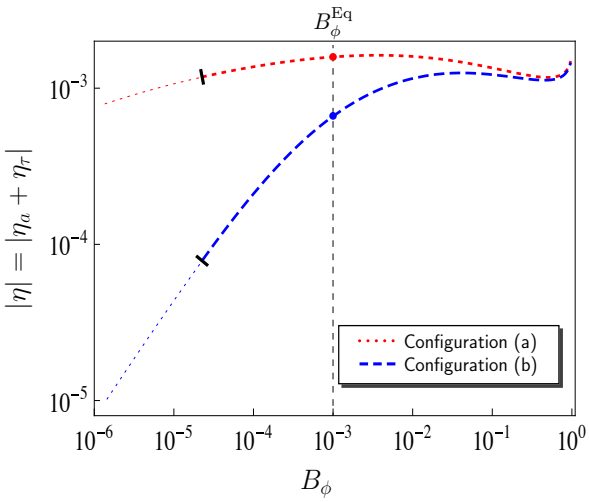

Figure 11: *Efficiency as a function of B_ϕ for $m_\Delta = 10^9$ GeV and $\tilde{m}_\Delta = 10^{-2}$ eV. Configuration (a) corresponds to $B_{\ell_{aa}} = B_{\ell_{a\tau}} = 0$ (i.e. $R = 0$) while configuration (b) corresponds to $B_{\ell_{aa}} = B_{\ell_{\tau\tau}}/99 = (1 - B_\phi)/100$ (i.e. $R \simeq 10^{-2}$). The lines are cut when the 2-flavor regime condition ceases to be fulfilled (see Sec. 3.2).*

We have seen in the previous sections that the efficiency strongly depends on the flavor parameters $B_{\ell_{ij}}$. Explicitly, we have shown that the efficiency has a minimum at $R \approx 3/4$, global maxima at $B_{\ell_{aa}} = B_{\ell_{a\tau}} \approx 0$ and $B_{\ell_{\tau\tau}} = B_{\ell_{a\tau}} \approx 0$, and a local maximum at $B_{\ell_{aa}} = B_{\ell_{\tau\tau}} \approx 0$. However, a maximal efficiency does not imply a maximal $B - L$ asymmetry. Indeed, using Eq. (15), we can actually compute a general upper bound for the purely flavored CP asymmetry:

$$|\epsilon_{\Delta_\alpha}^{\ell(\not{F})}| \leq \frac{1}{2\pi}\, g(m_{\Delta_\alpha}^2/m_{\Delta_\beta}^2)\, \left[\sqrt{B_{aa}^\ell B_{\tau\tau}^\ell} + \sqrt{B_{a\tau}^\ell\,(B_{aa}^\ell + B_{\tau\tau}^\ell)}\right] , \tag{86}$$

where we assumed perturbative Yukawa couplings for the second triplet generation, i.e. $|Y_\beta| \leq 1$. This expression shows clearly that the three configurations that maximize the efficiency give vanishing CP asymmetries! This can be understood easily from the fact these configurations involve a Yukawa coupling only for one flavor. We see also that the upper bound on the CP asymmetry is directly related to the hierarchy between the different triplet masses, which is compatible with the requirement in Eq. (84), i.e. a smooth triplet mass hierarchy favors PFL scenario and allows for a large CP asymmetry.

We plot in Fig. 12 the resulting maximal $B-L$ final asymmetry that can be achieved, as a function of the flavor parameter R, for $m_{\Delta_\alpha}/m_{\Delta_\beta} = 10^{-1}$. To this end we have considered the same parameter configuration used in Fig. 8. It can be seen that the maximal $B - L$ asymmetry that can be achieved can account for the observed baryon asymmetry of the Universe for a large range of R values, except at $R \approx 3/4$. We also point out that, if the neutrino mass matrix is dominated by the light scalar triplet, the constraints coming from neutrino data are compatible with successful PFL scenario. One realizes as well that two of the $B-L$ asymmetry global maxima are shifted with respect to

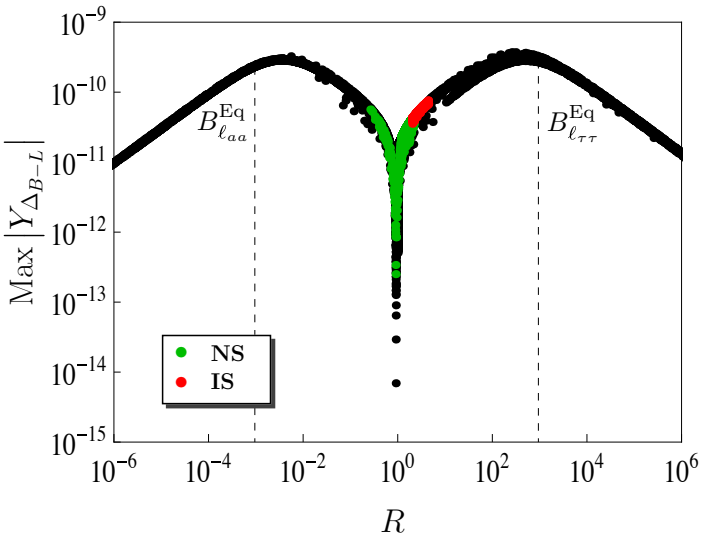

Figure 12: *Maximum attainable final $B-L$ asymmetry as a function of the R parameter, for $m_{\Delta_\alpha} = 10^9$ GeV, $m_{\Delta_\beta} = 10^{10}$ GeV, $\tilde{m}_\Delta = 10^{-2}$ eV and $B_\phi = 10^{-4}$. Neutrino data constraints have been imposed as in Fig. (8).*

the efficiency maxima, and are now located around the points at which $\ell_i \ell_i \to \bar{\Delta}$ inverse decay rates are of the order of the Universe Hubble expansion rate, where $B_{\ell_{ii}} = B^{\rm Eq}_{\ell_{ii}}$, see Eq. (77). As a final remark, it is worth noting that the local maximum at $R \approx 1$ has gone away.

This result has to be compared with the unflavored case, where the CP asymmetry is very suppressed for $B_\phi \ll B_\ell$ or $B_\phi \gg B_\ell$, since the CP asymmetry is proportional to $\sqrt{B_\phi B_\ell}$—see Eqs. (14) and (19). This is no more the case in PFL leptogenesis, since the lepton number conserving and flavor violating CP asymmetries depend only on Yukawa couplings.

5 General triplet flavored leptogenesis

Having discussed the viability of the PFL scenario in pure type-II seesaw models, we are now in a position to analyze the impact that flavor effects may have in general triplet flavored leptogenesis models. Here, as already defined in the introduction, by "general models" we refer to models where the lepton number violating CP asymmetries are relevant or even dominate over the lepton number conserving CP asymmetries which drive PFL. Accordingly, if the extra degrees of freedom enabling a non-vanishing CP asymmetry are additional triplets, a general model will be defined by Eq. (13), while if the extra degrees of freedom are RH neutrinos—as will be the case in models featuring interplay between type-I and type-II seesaws—the CP asymmetry in Eq. (21), being lepton number violating, will always define a "general model". In what follows we will assume the asymmetry is entirely generated via the decays of the lightest triplet, something that can be achieved

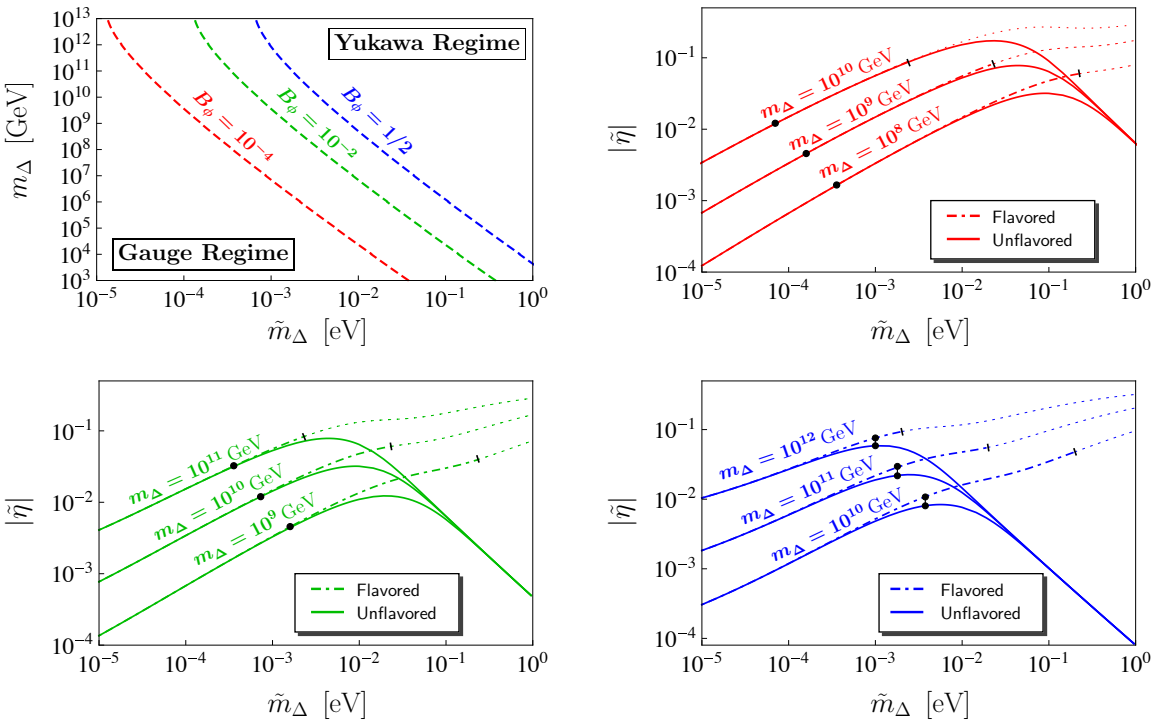

Figure 13: *Upper left-hand side plot: Yukawa and gauge regimes for different values of B_ϕ in the plane $m_\Delta - \tilde{m}_\Delta$. The remaining plots show the dependence of the efficiency-like parameter $\tilde{\eta}$ (for the unflavored case $\tilde{\eta}$ refers to the efficiency) with the effective mass parameter $\tilde{m}_\Delta$, for $B_\phi = 10^{-4}$ (upper right-hand side plot), $B_\phi = 10^{-2}$ (lower left-hand side plot) and $B_\phi = 1/2$ (lower right-hand side plot). We fixed $\bar{\epsilon}_\Delta = 0$ and the flavor configuration according to $B_{\ell_{aa}} = B_{\ell_{a\tau}} = 0$ and $B_{\ell_{\tau\tau}} = 1 - B_\phi$. Black dots correspond to $\tilde{m}_\Delta = \tilde{m}^*_\Delta$. The lines are cut when the 2-flavor regime condition ceases to be fulfilled (see Sec. 3.2).*

by taking a heavy mass spectrum obeying the following hierarchy: $m_\Delta \ll M_{\Delta_\alpha, N_\alpha}$.

In "general" scenarios, since the CP asymmetries are lepton number breaking, successful leptogenesis is possible in the absence of lepton flavor effects, in contrast to PFL where flavor effects are mandatory. In what follows we will quantify the enhancement that the inclusion of flavor effects may have in the final $B - L$ asymmetry, and in order to do that and to put the discussion in context we will start by briefly reviewing some general well known results of the unflavored regime, which have been derived from kinetic equations in which none of the SM reactions were taken into account (see Sec. 3.1) [11].

In the unflavored case, an efficiency function accounting for the z (temperature) evolution of the unflavored $B - L$ asymmetry can be defined[13]:

$$\eta(z) = -\frac{Y_{\Delta_{B-L}}(z)}{\epsilon_\Delta \, Y_\Sigma^{\rm Eq}(z_0)} \ , \tag{87}$$

[13]With the procedure followed in Sec. 3.3, but using instead the system of equations in (30) and (31), an explicit expression for $\eta(z)$ can be derived for the unflavored regime.

where at freeze out $\eta \equiv \eta(z \to \infty)$. As in fermion triplet leptogenesis, in this case one can also define a gauge and a Yukawa regime, which boundaries in the $\tilde{m}_\Delta - m_\Delta$ parameter space plane are determined by the values of B_ϕ, as displayed in Fig. 13 (upper left-hand side plot). While in the gauge regime triplet dynamics is dominated by gauge-mediated triplet annihilation, in the Yukawa regime the dynamics is driven by Yukawa-induced reactions, and so it is in the latter where flavor effects can have striking implications. For a fixed triplet mass, the transition between both regimes becomes determined by a "critical" $\tilde{m}_\Delta$, that we denote by $\tilde{m}^\star_\Delta$ [14].

The behavior of the efficiency (i.e. of the $B - L$ asymmetry) is to a large extent determined by the regime where leptogenesis takes place (gauge or Yukawa), or in other words by the location of the boundary in the $\tilde{m}_\Delta - m_\Delta$ plane, determined in turn by the value of B_ϕ. For the parameter space points shown in Fig. 13 (upper left-hand side plot), the behavior of the $B - L$ asymmetry goes along the following lines:

- *The $B_\phi = 1/2$ case*:
  In the gauge (Yukawa) regime the asymmetry increases (decreases) with $\tilde{m}_\Delta$. In the gauge regime this is due to the fact that there is no substantial production of the asymmetry until z approaches the value $z = z_A$ where γ_A/γ_D goes below unity, $z_A \sim 3$ in the right-hand side plot in Fig. 3. The generation of the $B - L$ asymmetry can then be understood as proceeding in two stages determined by two z (temperature) windows: $z < z_A$ and $z > z_A$. For $z < z_A$ the $B - L$ asymmetry is suppressed by a factor $\gamma_D/\gamma_A \propto m_\Delta \tilde{m}_\Delta/g^4$, so for a fixed scalar triplet mass the smaller $\tilde{m}_\Delta$, the smaller the ratio γ_D/γ_A, and so the asymmetry produced. In this range most of the production occurs when $z \lesssim z_A$. Before, γ_D/γ_A is exponentially suppressed. For $z > z_A$ instead, γ_A becomes irrelevant and, since in the gauge regime there is no suppression effect from inverse decays, the asymmetry produced within this z range is simply equal to the number of triplets left times the CP asymmetry, $Y_{\Delta_{B-L}} \simeq \epsilon_\Delta Y^{\rm Eq}_\Delta(z \sim z_A)$. The relevance of this contribution is determined by $\tilde{m}_\Delta$: large values of this parameter imply small values for z_A, which then in turn imply a less Boltzmann suppressed $Y^{\rm Eq}_\Delta(z_A)$. Thus, the $B - L$ asymmetry generated consist of two contributions, one generated at $z < z_A$ and a second produced at $z > z_A$, namely

$$Y_{\Delta_{B-L}} \simeq \epsilon_\Delta \int_{z_0}^{z_A} \frac{dY^{\rm Eq}_\Sigma}{dz} \frac{\gamma_D}{4\gamma_A} dz + \epsilon_\Delta Y^{\rm Eq}_\Sigma(z_A) \simeq \epsilon^\ell_\Delta Y^{\rm Eq}_\Sigma(z_A)(z_A/4 + 1) \; . \tag{88}$$

  In the Yukawa regime instead, the efficiency decreases with $\tilde{m}_\Delta$ because in this case still there is no substantial asymmetry produced until z approaches z_A, and because the asymmetry produced afterwards is further washed-out by the inverse decay whose magnitude increases with $\tilde{m}_\Delta$.

[14] In practice, for a given value of m_Δ, $\tilde{m}^\star_\Delta$ is defined as the value of $\tilde{m}_\Delta$ above (below) which the inverse decays are (not) in thermal equilibrium once the gauge scatterings cease to dominate the whole process (i.e. it leads to $\gamma_D/n^{\rm Eq}_\Delta H = 1$ when γ_A goes below γ_D at a temperature $z = z_A$). Note that $\tilde{m}^\star_\Delta$ and $\tilde{m}^{\rm eff}_\Delta$, defined in Eq. (49), are unrelated parameters.

- *The small B_ϕ case ($B_\phi = 10^{-2}$ or $B_\phi = 10^{-4}$)*:
  As can be seen in the upper right-hand and lower left-hand plots in Fig. 13 the efficiency goes on to increase with $\tilde{m}_\Delta$ well inside the Yukawa regime. This can be understood from the fact that in this case, even if the total decay rate is well in thermal equilibrium and faster than the gauge scattering rate, the decay to a pair of scalars remains out-of-equilibrium (see Fig. 3, left-hand side plot), which implies that lepton number is not broken by inverse decay, resulting in no washout from these processes. The efficiency is suppressed only by gauge-mediated triplet scatterings which, as pointed out in the previous item, precludes any substantial production of $B-L$ asymmetry until z reaches $\sim z_A$. All in all, despite standing in the Yukawa regime, the $B-L$ asymmetry is only suppressed by gauge scatterings in the way stressed in the previous item, and so the total $B-L$ asymmetry is again given by Eq. (88). For large values of $\tilde{m}_\Delta$, the gauge suppression is nevertheless faint because z_A is not much larger than unity. This results in very large efficiency for $B_\phi \ll 1/2$. Only when $\tilde{m}_\Delta \gg \tilde{m}_\Delta^\star$ is lepton number effectively broken by scalar doublet-triplet inverse decays and the efficiency decreases with $\tilde{m}_\Delta$. Note that, even if large efficiencies can be obtained in this way for $B_\phi \ll 1/2$, since lepton number is unbroken in the $B_\phi \to 0$ limit, these efficiency enhancements are accompanied by a suppression of the CP asymmetry, so that still the maximum $B-L$ asymmetry is obtained for values of B_ϕ not far from its maximum value $1/2$.

The picture described in the items above is expected to change as soon as one hits the flavor regime, if the parameters are such that triplet dynamics takes place in the Yukawa regime. In order to discuss the impact that flavor effects may have, it is convenient to introduce an efficiency-like parameter. Let us discuss this in some more detail. Flavor coupling does not allow a conventional definition of an efficiency, however a parameter resembling the efficiency of the unflavored case can be defined:

$$\tilde{\eta} = -\frac{Y_{\Delta_{B-L}}(z\to\infty)}{\epsilon_\Delta Y_\Sigma^{\rm Eq}(z_0)} \ , \tag{89}$$

with $\tilde{\eta}$ given by

$$\tilde{\eta} \equiv \frac{1}{2}\left[(\eta_{aa}+\eta_{a\tau}+\eta_{\tau a}+\eta_{\tau\tau}) + \bar{\epsilon}_\Delta\,(\eta_a+\eta_\tau)\right] \ , \tag{90}$$

where the flavored efficiency functions have been defined in Eq. (68) and with

$$\epsilon_\Delta = \epsilon_\Delta^{\ell_a} + \epsilon_\Delta^{\ell_\tau} \qquad \text{and} \qquad \bar{\epsilon}_\Delta = \frac{\epsilon_\Delta^{\ell_a} - \epsilon_\Delta^{\ell_\tau}}{\epsilon_\Delta} \ . \tag{91}$$

Note that the definition of $\tilde{\eta}$ is such that when taking the limit $\epsilon_\Delta^{\ell_a} \to \epsilon_\Delta^{\ell_\tau}$, one recovers the usual definition of the efficiency. This parameter proves to be useful in particular when comparing the results obtained in the flavored regime with those arising from the unflavored limit. Instead, the parameter $\bar{\epsilon}_\Delta$, introduced in the definition of $\tilde{\eta}$, has a two-fold utility: first of all it "measures" the deviation from the PFL ($\bar{\epsilon}_\Delta \gg 1$) and the general

scenarios ($\bar{\epsilon}_\Delta \ll 1$); secondly, it "measures" the flavor misalignment of the source terms in the evolution equations of the $B/3 - L_i$ charges.

In order to quantify the impact that flavor effects have on the $B - L$ asymmetry, it is useful to consider first a case where both CP flavored asymmetries are equal, i.e. $\bar{\epsilon}_\Delta = 0$, that is to say in a way the extreme opposite to the PFL case. This will allow to discuss flavor effects that are different from the ones we discussed in the previous section for the PFL case. For this case, we show in Fig. 13 the efficiency-like parameter $\tilde{\eta}$ as a function of $\tilde{m}_\Delta$ for different values of (m_Δ, B_ϕ), overlapped with the results we got for the unflavored case.

Some comments are in order regarding these results. Either in the gauge or in the Yukawa regime (for $\tilde{m}_\Delta \sim \tilde{m}^\star_\Delta$), gauge scatterings preclude any substantial creation of a $B - L$ asymmetry as long as $\gamma_A/\gamma_D \gg 1$, that is to say as long as z is below $\sim z_A$. The $B/3 - L_i$ asymmetry production is anyway suppressed by a γ_D/γ_A factor as in Eq. (88). Gauge scatterings, being flavor "blind", are insensitive to lepton flavor effects and so the suppressions they induce cannot be overcome. This means that, as long as we consider values of parameters which in the unflavored case gives Eq. (88) i.e. the maximum efficiency allowed by gauge scattering (in the gauge regime, or in the Yukawa regime for $B_\phi < 1/2$ and not too large values of $\tilde{m}$), flavor effects cannot further enhance the efficiency. However, in the Yukawa regime, for large values of $\tilde{m}_\Delta$, since inverse decay washouts are flavor sensitive, flavor effects allow to largely avoid this effect, so that the efficiency goes on to increase also there, as Fig. 13 shows. As a result in this case too, one is left only with the unavoidable gauge scattering suppression. This suppression is nevertheless very mild for large values of $\tilde{m}$ (i.e. small values of z_A). Hence, large enhancement of the efficiency can be obtained from flavor effects, especially for large values of B_ϕ. In other words, deep inside the Yukawa region ($\tilde{m}_\Delta \gg \tilde{m}^\star_\Delta$) where gauge scattering suppression is faint, flavor effects start showing up and become even striking as $\tilde{m}_\Delta$ increases and B_ϕ approaches $1/2$. Summarizing, in this equal flavored CP asymmetries case we consider here ($\bar{\epsilon}_\Delta = 0$), Eq. (88) can still be used as an approximate upper bound of the $B - L$ asymmetry one can reach in all regimes, even deep in the Yukawa regime. We have checked that this upper bound can be saturated in all regimes up to a factor ~ 2.

To further emphasize the effects of flavor in the $\bar{\epsilon}_\Delta = 0$ case, we have calculated the efficiency-like parameter $\tilde{\eta}$ as a function of B_ϕ. The calculation has been done for fixed parameters m_Δ and $\tilde{m}_\Delta$, and for two flavor configurations (a)—the one already used in Fig. 11—and (c) which corresponds to $B_{\ell aa} = B_{\ell\tau\tau} = (1 - B_\phi)/2$, i.e. without any flavor structure. The results are displayed in Fig. 14 (left-hand side plot), where the flavored and unflavored (as e.g. in Refs. [11, 15]) outputs are compared. It can be seen that considering only the effects of the SM interactions (i.e. configuration (c)), one can get an enhancement of order 2 with respect to the unflavored case, whereas for the flavor configuration (a) one can get a further one-order of magnitude enhancement, as can be seen in particular for $B_\phi = B_\ell = 1/2$.

Finally, let us discuss what happens very qualitatively in cases other than the pure PFL case, $\epsilon^{\ell_\tau}_\Delta = -\epsilon^{\ell_a}_\Delta$ and the "opposite" case, $\epsilon^{\ell_\tau}_\Delta = \epsilon^{\ell_a}_\Delta$. In these "intermediate" cases the "efficiency" as defined in Eq. (89) cannot be considered as an efficiency anymore, because

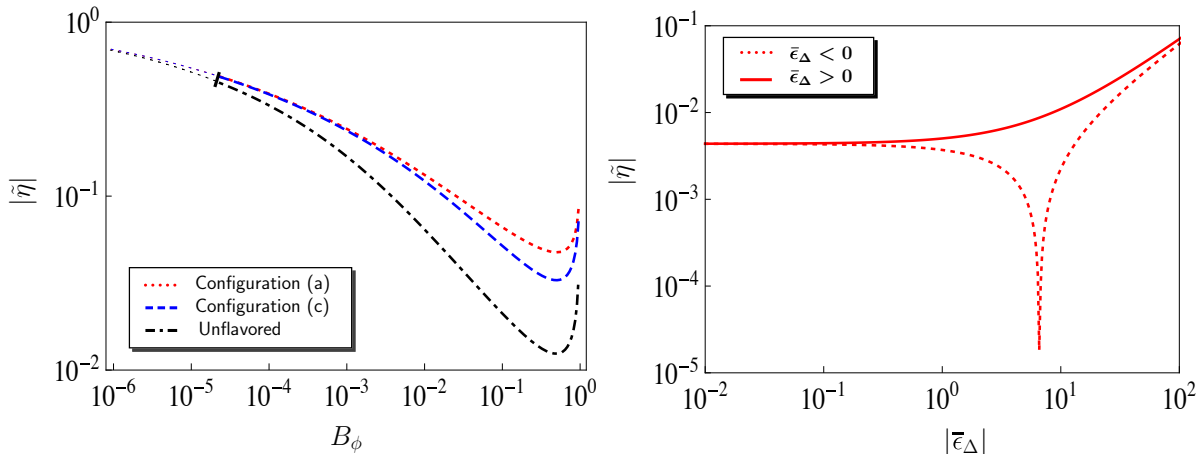

Figure 14: *Left-hand plot: Efficiency-like parameter $\tilde{\eta}$ as a function of B_ϕ, for $\epsilon^{\ell_a}_\Delta = \epsilon^{\ell_\tau}_\Delta$. The flavor configuration (a) corresponds to the one used in Fig. 11, while (c) corresponds to $B_{\ell aa} = B_{\ell\tau\tau} = (1 - B_\phi)/2$ (for the unflavored case $\tilde{\eta}$ refers to the efficiency). Right-hand plot: Efficiency-like parameter $\tilde{\eta}$ as a function of $|\bar{\epsilon}_\Delta|$ for $B_\phi = 1/2$ and flavor configuration (a). In both plots we fixed $m_\Delta = 10^{11}\,GeV$ and $\tilde{m}_\Delta = 10^{-2}$ eV. The lines are cut whenever the 2-flavor regime condition ceases to be fulfilled (see Sec. 3.2).*

it can be larger than one. For instance in the pure PFL case it is infinity since $\epsilon_\Delta = 0$. As a result it is difficult to span the range of possibilities in simple terms for these cases. To get a reliable idea of the behavior of the efficiency-like parameter, and thus of the $B - L$ asymmetry, in a specific case, the most efficient procedure is probably to integrate first the full set of Boltzmann equations in a "blind" way and see what the result looks like before trying to understand it by simple means. But the basic picture qualitatively remains clear. As long as $z < z_A$ any flavor asymmetry production is suppressed by a factor of γ_D/γ_A, and afterwards the $B - L$ asymmetry that can be produced can anyway not be larger than the number of triplets remaining at $z \sim z_A$ times the sum of the absolute values of the flavor asymmetries. The important flavor effects stressed above, from the L-violating inverse decays as well as from the L-violating decays, will be operative in a way which may depend non trivially on basically all parameters, the flavor CP asymmetries, the $C^{\ell,\phi}$ constants, the total decay rate and the various branching ratios.

As an illustration of the efficiency dependence on the mismatch between the flavored CP asymmetries, parameterized by $\bar{\epsilon}_\Delta$, on the right-hand side plot in Fig. 14 we show the dependence of $\tilde{\eta}$ with $\bar{\epsilon}_\Delta$ for $B_\phi = 1/2$ for the flavor configuration (a). In the region where $\bar{\epsilon}_\Delta \ll 1$ is small ($\epsilon^{\ell_a}_\Delta \sim \epsilon^{\ell_\tau}_\Delta$), as previously stressed, any possible mismatch between the asymmetries in flavor a and τ can only be due to the flavor dependence of the washout terms. As $\bar{\epsilon}_\Delta$ increases, the source terms start having a flavor dependence as well, and so an imbalance between production in flavor a and τ appears. The flavor dependence of both production and washout at large $\bar{\epsilon}_\Delta$, yields larger values for $\tilde{\eta}$. In other words, flavor effects are diminished in those regions of parameter space where $\bar{\epsilon}_\Delta \ll 1$ and become more remarkable in regions where $\bar{\epsilon}_\Delta \gg 1$. Accordingly, in the various flavor

regimes, enhancements of the efficiency-like parameter $\tilde{\eta}$ with respect to the unflavored case are a consequence of combined effects: the mismatch between the different flavored CP asymmetries $\epsilon_{\Delta}^{\ell_i}$, the SM interactions through the C^{ℓ} and C^{ϕ} matrices, and the flavor configurations encoded in $B_{\ell_{ij}}$.

6 Conclusions

We have considered scalar triplet leptogenesis scenarios where the states enabling successful production of the cosmic baryon asymmetry are either extra triplets or RH neutrinos. We have derived for the first time the complete set of flavored classical Boltzmann equations governing the evolution of the different relevant asymmetries, including the effects of those SM reactions which in the leptogenesis era may be fast: charged lepton and quark Yukawa reactions as well as QCD and electroweak sphaleron processes. The resulting network of kinetic equations combined with the different *asymmetry coupling matrices*, which follow from the chemical equilibrium conditions enforced by the fast SM processes, provide the tools for studying triplet scalar leptogenesis in full generality. Furthermore, by requiring that the decoherence rate to be faster than the leptonic inverse decay rate during the leptogenesis era, we determined the domain of validity of the various flavor regimes.

In scenarios involving an additional triplet (purely type-II seesaw scenarios), we have identified a novel class of models where the flavored CP asymmetries, consisting of lepton number violating and lepton number conserving contributions, become dominated by the lepton number conserving piece. Such a dominance naturally shows up as soon as the couplings of at least one triplet (i.e. not necessarily of all seesaw states as for PFL type-I seesaw scenarios) approximately conserve L, in practice simply that it couples more to leptons than to scalars. The purely flavored CP asymmetries have no reasons to be suppressed by the smallness of the light neutrino masses since, in contrast to the lepton-number-violating CP asymmetries, they only involve L-conserving couplings.

With the aid of the derived flavored Boltzmann equations and *asymmetry coupling matrices*, we have carried out a throughout study of the PFL scenario in the two flavor regime, for definitiveness. The way this PFL scenario works is totally novel (for small values of B_{ϕ} which gives natural dominance of the purely flavored CP asymmetries): in this case there is no L-violating process in thermal equilibrium at any epoch but yet flavor effects do allow the creation of a $B-L$ asymmetry from the L-violating slow decay of the triplet to SM scalars. We have proved its viability by calculating the $B-L$ yield, finding that, for utterly reasonable and wide ranges of parameter values, a baryon asymmetry consistent with observation can always be achieved. By exploring the $B-L$ asymmetry parameter space dependence, we have determined the lepton flavor configuration that maximizes the efficiency, finding that the same structure renders the flavored CP asymmetry minimal. Our findings show that maximal $B-L$ yield is achieved for intermediate lepton flavor configurations.

Finally, we discussed general scenarios, which we have defined by the condition of

the CP asymmetry involving lepton number violation. These scenarios can arise either in models with extra triplets or with RH neutrinos (models exhibiting interplay between type-I and type-II seesaw). We discussed the impact that lepton flavor effects may have in the final $B-L$ asymmetry, showing that relevant flavor effects can only be achieved in the Yukawa regime, being more striking as deeper one moves into that regime, and depending on the parameter flavor configuration. Our results show that for certain flavor structures—once lying in the Yukawa regime—the asymmetry may be enhanced by several orders of magnitude. In both regimes, the $B-L$ asymmetry production is suppressed as long as the gauge scattering rate is faster than the decay rate (i.e. for $z \ll z_A$), and the asymmetry produced afterwards is proportional to the number of triplet remaining afterwards. The latter being Boltzmann suppressed if $z_A > 1$, the suppression is more pronounced for smaller values of m_Δ, given that as m_Δ decreases z_A increases. Deep in the Yukawa regime, however, the decay rate becomes faster than the gauge scattering rate at very early epochs, $z_A \lesssim 1$ and this Boltzmann suppression goes away. In this way, deep in the Yukawa regime, one can basically avoid all efficiency suppressions, from gauge scattering as well as, through flavor effects, from L-violating inverse decays.

7 Acknowledgements

We want to thank Enrico Nardi for many stimulating discussions and valuable comments. DAS wants also to thanks Juan Racker for useful comments. DAS is supported by the Belgian FNRS agency through a "Chargé de Recherches" contract and will like to thank the "Service de Physique Théorique" of the "Université Libre de Bruxelles" for the warm hospitality during the completion of this work. The work of MD and TH is supported by the FNRS, the IISN and by the Belgian Science Policy, IAP VII/37.

A Conventions and definitions

Here in this appendix we collect all the relevant formulæ we used throughout the paper. We stress we have used Maxwell-Boltzmann distributions, so for the number of relativistic degrees of freedom we have used $g_\star = \sum_{i=\text{All species}} g_i = 118$ ($T \gg 300$ GeV) while for the entropy density

$$s(z) = \frac{4 m_\Delta^3 g_\star}{z^3 \pi^2} \ , \tag{92}$$

with $z = m_\Delta / T$. For the expansion rate of the Universe we used

$$H(z) = \sqrt{\frac{8 g_\star}{\pi}} \frac{m_\Delta^2}{M_{\text{Planck}}} \frac{1}{z^2} \ . \tag{93}$$

Decay and scattering $1 \leftrightarrow 2$ and $2 \leftrightarrow 2$ reaction densities are given by:

$$\gamma_D = \frac{K_1(z)}{K_2(z)} \, n_\Sigma^{\text{Eq}} \, \Gamma_\Delta^{\text{Tot}} \ , \tag{94}$$

$$\gamma_S = \frac{m_\Delta^4}{64\,\pi^4}\int_{x_{\rm min}}^{\infty} dx\sqrt{x}\,\frac{K_1(z\sqrt{x})\,\widehat{\sigma}_S}{z}\ . \tag{95}$$

Here $n_\Sigma^{\rm Eq}$ is the $\Sigma = \Delta + \Delta^\dagger$ number density (number density for a non-relativistic species), $x = s/m_\Delta^2$ (s being the center-of-mass energy), $\Gamma_\Delta^{\rm Tot}$ denotes the triplet total decay width, given in Eq. (10), whereas $\widehat{\sigma}_S$ the reduced cross section. The integration upper and lower limits are determined by the kinematics of the corresponding scattering process: for gauge boson mediated processes $x_{\rm min} = 4$, for Yukawa (or scalar) induced reactions $x_{\rm min} = 0$.

Denoting $\delta = \Gamma_\Delta^{\rm Tot}/m_\Delta$, we have found that the reduced cross sections for the s and t channel $\Delta L = 2$ processes can be written as:

$$\begin{aligned}
\widehat{\sigma}_{\ell_i\ell_j}^{\phi\phi} &= 64\pi\,B_\phi\,B_{\ell_{ij}}\,\delta^2\,\frac{x}{(x-1)^2+\delta^2}\ ,\\
\widehat{\sigma}_{\phi\ell_i}^{\phi\ell_j} &= 64\pi\,B_\phi\,B_{\ell_{ij}}\,\delta^2\,\frac{1}{x}\left[\ln(1+x) - \frac{x}{1+x}\right]\ .
\end{aligned} \tag{96}$$

The reduced cross sections for the s and t channel flavor violating reactions, instead, can be written according to:

$$\begin{aligned}
\widehat{\sigma}_{\ell_i\ell_j}^{\ell_n\ell_m} &= 64\pi\,B_{\ell_{nm}}\,B_{\ell_{ij}}\,\delta^2\,\frac{x^2}{(1-x)^2+\delta^2}\ ,\\
\widehat{\sigma}_{\ell_i\ell_n}^{\ell_j\ell_m} &= 64\pi\,B_{\ell_{nm}}\,B_{\ell_{ij}}\,\delta^2\,\left[\frac{x+2}{x+1} - \ln(1+x)\right]\ .
\end{aligned} \tag{97}$$

Finally, the reduced cross section for gauge induced processes reads [11, 15, 44]

$$\begin{aligned}
\widehat{\sigma}_A =& \frac{2}{72\pi}\left\{(15C_1 - 3C_2)\,r + (5C_2 - 11C_1)\,r^3\right.\\
&\left. +3\left(r^2-1\right)\left[2C_1 + C_2\left(r^2-1\right)\right]\ln\left(\frac{1+r}{1-r}\right)\right\} + \left(\frac{50g^4 + 41g'^4}{48\pi}\right)\,r^{3/2}\ ,
\end{aligned} \tag{98}$$

where the following notation has been adopted: $r = \sqrt{1-4/x}$ and $C_1 = 12g^4 + 3g_Y^4 + 12g^2g_Y^2$ and $C_2 = 6g^4 + 3g_Y^4 + 12g^2g_Y^2$ (with g and g_Y the $SU(2)$ and $U(1)$ SM gauge coupling constants).

The reaction densities with a resonant intermediate state subtracted can be calculated from Eqs. (94), (95), (96) and (97) as follows:

$$\begin{aligned}
\gamma'^{\phi\phi}_{\ell_i\ell_j} &= \gamma^{\phi\phi}_{\ell_i\ell_j} - B_{\ell_{ij}}\,B_\phi\,\gamma_D\ ,\\
\gamma'^{\ell_n\ell_m}_{\ell_i\ell_j} &= \gamma^{\ell_n\ell_m}_{\ell_i\ell_j} - B_{\ell_{ij}}B_{\ell_{nm}}\gamma_D\ .
\end{aligned} \tag{99}$$

Rates for the different SM reactions are approximately given by [38, 39, 45, 46]:

$$\text{QCD instantons:}\qquad \gamma_{\rm QCD}(T) \simeq 312\,\alpha_{\rm S}\,T^4\ , \tag{100}$$

$$\text{Electroweak sphalerons:}\qquad \gamma_{\rm EW}(T) \simeq 26\,\alpha_{\rm EW}\,T^4\ , \tag{101}$$

$$\text{Yukawa reactions:}\qquad \gamma_{f_i}(T) \simeq 5\times10^{-3}\,h_{f_i}^2\,T\,n_{f_i}^{\rm Eq} = 5\times10^{-4}\,h_{f_i}^2\,T^4\ , \tag{102}$$

where h_{f_i} denotes the Yukawa coupling of fermion f_i.

B Summary of the different C^ℓ and C^ϕ matrices

B.1 C^ℓ matrices in all possible regimes

As it has been discussed in Sec. 3.2, in scalar triplet flavored leptogenesis there are parameter space configurations for which lepton flavor coherence is not lost when the SM tau Yukawa reaction (or any other SM lepton Yukawa interaction) becomes fast. In those cases, the C^ℓ and C^ϕ matrices certainly differ from those derived in Sec. 3.1, which hold when lepton flavor decoherence takes place at the same temperature at which the corresponding SM Yukawa coupling becomes fast. Although this lepton flavor decoherence "delay" is not inherent to scalar triplet flavored letogenesis, and it is rather a consequence of parameter choices, here we summarize all possible C^ℓ and C^ϕ matrices including as well those cases. The list presented here thus encompasses all the scenarios one can consider when tracking the $B-L$ asymmetry in triplet scalar flavored leptogensis scenarios.

Tab. 1 displays the different possible temperature regimes, the corresponding reactions which are faster than the Hubble expansion rate, the lepton flavor regimes (one-, two- or three-flavor regimes) and the corresponding global symmetries of the early Universe effective Lagrangian. In Tab. 2, instead, we specify for the different temperature regimes the asymmetry charges for which kinetic evolution equations have to be written and the corresponding C^ℓ and C^ϕ matrices valid in each case. We remind that $T^{f_i}_{\rm decoh}$, as defined in Sec. 3.2, refers to the temperature at which the lepton-related triplet inverse decay becomes smaller than the SM lepton f_i Yukawa interaction.

B.2 C^ℓ and C^ϕ matrices in the lepton one-flavor limit

- *QCD instantons, electroweak sphalerons, bottom, charm and tau Yukawa-related reactions in thermal equilibrium, $T \subset [10^9, 10^{12}]$ GeV*:
  Sticking to the one lepton flavor approximation means first choosing a direction in the $\tau - a$ flavor space. Taking either $B_{\ell_{aa}} = 1 - B_\phi$ or $B_{\ell_{\tau\tau}} = 1 - B_\phi$, both cases are governed by the system of equations in (24), (30) and (31) with the structure of the $C^{\ell,\phi}$ matrices determined by the corresponding choice. If $B_{\ell_{aa}} = 1 - B_\phi$, the asymmetry is entirely projected along the a flavor direction and so the one lepton flavor approximation $C^{\ell,\phi}$ matrices are given by

$$C^\ell = \begin{pmatrix} -6/359 & 307/718 \end{pmatrix} \ , \qquad C^\phi = \begin{pmatrix} 258/359 & 41/359 \end{pmatrix} \ . \tag{103}$$

  If instead the asymmetry is projected along the τ flavor the matrices read:

$$C^\ell = \begin{pmatrix} 39/359 & 117/359 \end{pmatrix} \ , \qquad C^\phi = \begin{pmatrix} 258/359 & 56/359 \end{pmatrix} \ . \tag{104}$$

- *Strange and muon Yukawa interactions in thermal equilibrium, $T \subset [10^5, 10^9]$ GeV:*
  Since in this regime the flavor basis is completely defined, there are several flavor projections which render flavor alignment. The corresponding $C^{\ell,\phi}$ matrices for the

T (GeV)	In equilibrium	Flavor(s)	Global symmetries of the effective $\mathcal{L}$
$\gtrsim 10^{15}$	Hyp.	1	$U(1)_Y \times U(1)_B \times U(1)_{E_R} \times U(1)_{PQ} \times$ $SU(3)_Q \times SU(3)_u \times SU(3)_d \times SU(3)_e$
$[10^{12}, 10^{15}]$	Hyp., t	1	$U(1)_Y \times U(1)_B \times U(1)_{E_R} \times$ $SU(2)_Q \times SU(2)_u \times SU(3)_d \times SU(3)_e$
$[10^9, 10^{12}]$:			
$[T^\tau_{\rm decoh}, 10^{12}]$	Hyp., Sphal., t,b,c	1	$U(1)_Y \times U(1)_Q \times U(1)_u \times SU(2)_d \times$ $SU(3)_e$
$[10^9, T^\tau_{\rm decoh}]$	Hyp., Sphal., t,b,c,τ	2	$U(1)_Y \times U(1)_Q \times U(1)_u \times SU(2)_d \times$ $SU(2)_e$
$[10^5, 10^9]$:			
$[T^\tau_{\rm decoh}, 10^9]$	Hyp., Sphal., t,b,c,s	1	$U(1)_Y \times U(1)_Q \times U(1)_u \times U(1)_d \times$ $SU(3)_e$
$[T^\mu_{\rm decoh}, T^\tau_{\rm decoh}]$	Hyp., Sphal., t,b,c,s,τ	2	$U(1)_Y \times U(1)_Q \times U(1)_u \times U(1)_d \times$ $SU(2)_e$
$[10^5, T^\mu_{\rm decoh}]$	Hyp., Sphal., t,b,c,s,τ,μ	3	$U(1)_Y \times U(1)_Q \times U(1)_u \times U(1)_d \times$ $U(1)_e$
$\lesssim 10^5$:			
$[T^\tau_{\rm decoh}, 10^5]$	Hyp., Sphal., t,b,c,s,u,d	1	$U(1)_Y \times SU(3)_e$
$[T^\mu_{\rm decoh}, T^\tau_{\rm decoh}]$	Hyp., Sphal., t,b,c,s,u,d,τ	2	$U(1)_Y \times SU(2)_e$
$[T^e_{\rm decoh}, T^\mu_{\rm decoh}]$	Hyp., Sphal., t,b,c,s,u,d,τ,μ	3	$U(1)_Y \times U(1)_e$
$\lesssim T^e_{\rm decoh}$	Hyp., Sphal., t,b,c,s,u,d,τ,μ,e	3	$U(1)_Y$

Table 1: *Temperature ranges and the corresponding reactions which are in thermal equilibrium. In the third column we show the number of flavor(s) that has (have) to be considered in the kinetic equations, and in the fourth column are the global symmetries of the early Universe effective Lagrangian are displayed.*

T (GeV)	Flavor(s)	C_ℓ	C_ϕ
$\gtrsim 10^{15}$	L	$\begin{pmatrix} 0 & \frac{1}{2} \end{pmatrix}$	$\begin{pmatrix} 3 & \frac{1}{2} \end{pmatrix}$
$[10^{12}, 10^{15}]$	L	$\begin{pmatrix} 0 & \frac{1}{2} \end{pmatrix}$	$\begin{pmatrix} 2 & \frac{1}{3} \end{pmatrix}$
$[10^9, 10^{12}]$:			
$[T^\tau_{\rm decoh}, 10^{12}]$	$B-L$	$\begin{pmatrix} 0 & \frac{3}{10} \end{pmatrix}$	$\begin{pmatrix} \frac{3}{4} & \frac{1}{8} \end{pmatrix}$
$[10^9, T^\tau_{\rm decoh}]$	$B/3 - L_{\tau,a}$	$\begin{pmatrix} -\frac{6}{359} & \frac{307}{718} & -\frac{18}{359} \\ \frac{39}{359} & -\frac{21}{718} & \frac{117}{359} \end{pmatrix}$	$\begin{pmatrix} \frac{258}{359} & \frac{41}{359} & \frac{56}{359} \end{pmatrix}$
$[10^5, 10^9]$:			
$[T^\tau_{\rm decoh}, 10^9]$	$B-L$	$\begin{pmatrix} 0 & \frac{3}{10} \end{pmatrix}$	$\begin{pmatrix} \frac{3}{4} & \frac{1}{8} \end{pmatrix}$
$[T^\mu_{\rm decoh}, T^\tau_{\rm decoh}]$	$B/3 - L_{\tau,a}$	$\begin{pmatrix} -\frac{6}{359} & \frac{307}{718} & -\frac{18}{359} \\ \frac{39}{359} & -\frac{21}{718} & \frac{117}{359} \end{pmatrix}$	$\begin{pmatrix} \frac{258}{359} & \frac{41}{359} & \frac{56}{359} \end{pmatrix}$
$[10^5, T^\mu_{\rm decoh}]$	$B/3 - L_{\tau,\mu,a}$	$\begin{pmatrix} -\frac{6}{179} & \frac{151}{358} & -\frac{10}{179} & -\frac{10}{179} \\ \frac{33}{358} & -\frac{25}{716} & \frac{172}{537} & -\frac{7}{537} \\ \frac{33}{358} & -\frac{25}{716} & -\frac{7}{537} & \frac{172}{537} \end{pmatrix}$	$\begin{pmatrix} \frac{123}{179} & \frac{37}{358} & \frac{26}{179} & \frac{26}{179} \end{pmatrix}$
$\lesssim 10^5$:			
$[T^\tau_{\rm decoh}, 10^5]$	$B/3 - L$	$\begin{pmatrix} 0 & \frac{3}{10} \end{pmatrix}$	$\begin{pmatrix} \frac{6}{11} & \frac{1}{11} \end{pmatrix}$
$[T^\mu_{\rm decoh}, T^\tau_{\rm decoh}]$	$B/3 - L_{\tau,a}$	$\begin{pmatrix} -\frac{3}{244} & \frac{209}{488} & -\frac{3}{61} \\ \frac{39}{488} & -\frac{33}{976} & \frac{39}{122} \end{pmatrix}$	$\begin{pmatrix} \frac{519}{976} & \frac{199}{1952} & \frac{31}{244} \end{pmatrix}$
$[T^e_{\rm decoh}, T^\mu_{\rm decoh}]$	$B/3 - L_{\tau,\mu,a}$	$\begin{pmatrix} -\frac{12}{481} & \frac{11}{26} & -\frac{2}{37} & -\frac{2}{37} \\ \frac{33}{481} & -\frac{1}{26} & \frac{35}{111} & -\frac{2}{111} \\ \frac{33}{481} & -\frac{1}{26} & -\frac{2}{111} & \frac{35}{111} \end{pmatrix}$	$\begin{pmatrix} \frac{256}{481} & \frac{1}{13} & \frac{4}{37} & \frac{4}{37} \end{pmatrix}$
$\lesssim T^e_{\rm decoh}$	$B/3 - L_{\tau,\mu,e}$	$\begin{pmatrix} \frac{9}{158} & \frac{221}{711} & -\frac{16}{711} & -\frac{16}{711} \\ \frac{9}{158} & -\frac{16}{711} & \frac{221}{711} & -\frac{16}{711} \\ \frac{9}{158} & -\frac{16}{711} & -\frac{16}{711} & \frac{221}{711} \end{pmatrix}$	$\begin{pmatrix} \frac{39}{79} & \frac{8}{79} & \frac{8}{79} & \frac{8}{79} \end{pmatrix}$

Table 2: *Temperature ranges, as in Tab. 1. In the second column, we show the asymmetries for which kinetic equations have to be written. In the third and fourth columns the different C^ℓ and C^ϕ matrices holding in each regime. Note that these matrices reduce to those found in the type-I seesaw case when removing their first column.*

alignments $B_{\ell_{ee}} = 1 - B_\phi$ and $B_{\ell_{\tau\tau}} = 1 - B_\phi$ (the results for $B_{\ell_{\mu\mu}} = 1 - B_\phi$ match those of $B_{\ell_{\tau\tau}} = 1 - B_\phi$) read:

$$B_{\ell_{ee}} = 1 - B_\phi : \quad C^\ell = \begin{pmatrix} -6/179 & 151/358 \end{pmatrix} \ , \quad C^\phi = \begin{pmatrix} 123/179 & 37/358 \end{pmatrix} \tag{105}$$

$$B_{\ell_{\tau\tau}} = 1 - B_\phi : \quad C^\ell = \begin{pmatrix} 33/358 & 172/537 \end{pmatrix} \ , \quad C^\phi = \begin{pmatrix} 123/179 & 26/179 \end{pmatrix} \tag{106}$$

- *All SM reactions in thermal equilibrium, $T \lesssim 10^5$ GeV:*
  In this case as well one can define a one-flavor approximation by fixing an alignment in flavor space. For $B_{\ell_{ii}} = 1 - B_\phi$ $(i = e, \mu, \tau)$ the $C^{\ell,\phi}$ matrices are given by

$$B_{\ell_{ii}} = 1 - B_\phi : \quad C^\ell = \begin{pmatrix} 9/158 & 221/711 \end{pmatrix} \ , \quad C^\phi = \begin{pmatrix} 39/79 & 8/79 \end{pmatrix} \ . \tag{107}$$

References

[1] D. V. Forero, M. Tortola and J. W. F. Valle, Phys. Rev. D **86**, 073012 (2012) [arXiv:1205.4018 [hep-ph]].

[2] M. C. Gonzalez-Garcia, M. Maltoni, J. Salvado and T. Schwetz, JHEP **1212**, 123 (2012) [arXiv:1209.3023 [hep-ph]].

[3] G. L. Fogli, E. Lisi, A. Marrone, D. Montanino, A. Palazzo and A. M. Rotunno, Phys. Rev. D **86**, 013012 (2012) [arXiv:1205.5254 [hep-ph]].

[4] G. Hinshaw *et al.* [WMAP Collaboration], arXiv:1212.5226 [astro-ph.CO].

[5] P. A. R. Ade *et al.* [Planck Collaboration], arXiv:1303.5076 [astro-ph.CO].

[6] P. Minkowski, *Phys. Lett.* B **67** 421 (1977); T. Yanagida, in *Proc. of Workshop on Unified Theory and Baryon number in the Universe*, eds. O. Sawada and A. Sugamoto, KEK, Tsukuba, (1979) p.95; M. Gell-Mann, P. Ramond and R. Slansky, in *Supergravity*, eds P. van Niewenhuizen and D. Z. Freedman (North Holland, Amsterdam 1980) p.315; P. Ramond, *Sanibel talk*, retroprinted as hep-ph/9809459; S. L. Glashow, in*Quarks and Leptons*, Cargèse lectures, eds M. Lévy, (Plenum, 1980, New York) p. 707; R. N. Mohapatra and G. Senjanović, *Phys. Rev. Lett.* **44**, 912 (1980); J. Schechter and J. W. F. Valle, Phys. Rev. D **22** (1980) 2227; Phys. Rev. D **25** (1982) 774.

[7] J. Schechter and J. W. F. Valle, Phys. Rev. D **22**, 2227 (1980); G. Lazarides, Q. Shafi and C. Wetterich, Nucl. Phys. B **181**, 287 (1981); R. N. Mohapatra and G. Senjanovic, Phys. Rev. D **23**, 165 (1981); C. Wetterich, Nucl. Phys. B **187**, 343 (1981);

[8] R. Foot, H. Lew, X. G. He and G. C. Joshi, Z. Phys. C **44**, 441 (1989).

[9] S. Davidson, E. Nardi and Y. Nir, Phys. Rept. **466**, 105 (2008) [arXiv:0802.2962 [hep-ph]].

[10] C. S. Fong, E. Nardi and A. Riotto, Adv. High Energy Phys. **2012**, 158303 (2012) [arXiv:1301.3062 [hep-ph]].

[11] T. Hambye, New J. Phys. **14**, 125014 (2012) [arXiv:1212.2888 [hep-ph]].

[12] E. Ma and U. Sarkar, Phys. Rev. Lett. **80**, 5716 (1998) [hep-ph/9802445].

[13] T. Hambye, E. Ma and U. Sarkar, Nucl. Phys. B **602** (2001) 23 [hep-ph/0011192].

[14] T. Hambye and G. Senjanovic, Phys. Lett. B **582**, 73 (2004) [hep-ph/0307237].

[15] T. Hambye, M. Raidal and A. Strumia, Phys. Lett. B **632**, 667 (2006) [hep-ph/0510008].

[16] T. Hambye, Y. Lin, A. Notari, M. Papucci and A. Strumia, Nucl. Phys. B **695**, 169 (2004) [hep-ph/0312203].

[17] D. Aristizabal Sierra, J. F. Kamenik and M. Nemevsek, JHEP **1010**, 036 (2010) [arXiv:1007.1907 [hep-ph]].

[18] D. Aristizabal Sierra, F. Bazzocchi and I. de Medeiros Varzielas, Nucl. Phys. B **858**, 196 (2012) [arXiv:1112.1843 [hep-ph]].

[19] R. Franceschini, T. Hambye and A. Strumia, Phys. Rev. D **78**, 033002 (2008) [arXiv:0805.1613 [hep-ph]].

[20] F. del Aguila and J. A. Aguilar-Saavedra, Nucl. Phys. B **813**, 22 (2009) [arXiv:0808.2468 [hep-ph]].

[21] A. Strumia, Nucl. Phys. B **809**, 308 (2009) [arXiv:0806.1630 [hep-ph]].

[22] G. C. Branco, R. G. Felipe and F. R. Joaquim, Rev. Mod. Phys. **84** (2012) 515 [arXiv:1111.5332 [hep-ph]].

[23] R. G. Felipe, F. R. Joaquim and H. Serodio, arXiv:1301.0288 [hep-ph].

[24] D. Aristizabal Sierra, M. Losada and E. Nardi, Phys. Lett. B **659**, 328 (2008) [arXiv:0705.1489 [hep-ph]].

[25] D. Aristizabal Sierra, L. A. Munoz and E. Nardi, Phys. Rev. D **80**, 016007 (2009) [arXiv:0904.3043 [hep-ph]].

[26] D. Aristizabal Sierra, M. Losada and E. Nardi, JCAP **0912**, 015 (2009) [arXiv:0905.0662 [hep-ph]].

[27] M. C. Gonzalez-Garcia, J. Racker and N. Rius, JHEP **0911**, 079 (2009) [arXiv:0909.3518 [hep-ph]].

[28] E. W. Kolb and S. Wolfram, Nucl. Phys. B **172**, 224 (1980) [Erratum-ibid. B **195**, 542 (1982)].

[29] S. Antusch and S. F. King, Phys. Lett. B **597**, 199 (2004) [hep-ph/0405093].

[30] A. Abada, P. Hosteins, F. -X. Josse-Michaux and S. Lavignac, Nucl. Phys. B **809**, 183 (2009) [arXiv:0808.2058 [hep-ph]].

[31] C. S. Fong, M. C. Gonzalez-Garcia and E. Nardi, JCAP **1102**, 032 (2011) [arXiv:1012.1597 [hep-ph]].

[32] J. McDonald, Phys. Rev. Lett. **88**, 091304 (2002) [hep-ph/0106249]; L. J. Hall, K. Jedamzik, J. March-Russell and S. M. West, JHEP **1003**, 080 (2010) [arXiv:0911.1120 [hep-ph]]; C. Cheung, G. Elor, L. J. Hall and P. Kumar, JHEP **1103**, 042 (2011) [arXiv:1010.0022 [hep-ph]]; C. E. Yaguna, JHEP **1108**, 060 (2011) [arXiv:1105.1654 [hep-ph]]; M. Frigerio, T. Hambye and E. Masso, Phys. Rev. X **1**, 021026 (2011) [arXiv:1107.4564 [hep-ph]]; X. Chu, T. Hambye and M. H. G. Tytgat, JCAP **1205**, 034 (2012) [arXiv:1112.0493 [hep-ph]].

[33] W. Buchmuller and M. Plumacher, Phys. Lett. B **511**, 74 (2001) [hep-ph/0104189].

[34] E. Nardi, Y. Nir, J. Racker and E. Roulet, JHEP **0601**, 068 (2006) [hep-ph/0512052].

[35] E. Nardi, J. Racker and E. Roulet, JHEP **0709**, 090 (2007) [arXiv:0707.0378 [hep-ph]].

[36] R. Barbieri, P. Creminelli, A. Strumia and N. Tetradis, Nucl. Phys. B **575**, 61 (2000) [hep-ph/9911315].

[37] J. A. Harvey and M. S. Turner, Phys. Rev. D **42**, 3344 (1990).

[38] G. D. Moore, Phys. Lett. B **412**, 359 (1997) [hep-ph/9705248].

[39] L. Bento, JCAP **0311**, 002 (2003) [hep-ph/0304263].

[40] E. Nardi, Y. Nir, E. Roulet and J. Racker, JHEP **0601**, 164 (2006) [hep-ph/0601084].

[41] S. Blanchet, P. Di Bari and G. G. Raffelt, JCAP **0703** (2007) 012 [hep-ph/0611337].

[42] A. Abada, S. Davidson, F. -X. Josse-Michaux, M. Losada and A. Riotto, JCAP **0604**, 004 (2006) [hep-ph/0601083].

[43] S. Antusch, P. Di Bari, D. A. Jones and S. F. King, Nucl. Phys. B **856**, 180 (2012) [arXiv:1003.5132 [hep-ph]].

[44] M. Cirelli, A. Strumia and M. Tamburini, Nucl. Phys. B **787**, 152 (2007) [arXiv:0706.4071 [hep-ph]].

[45] B. A. Campbell, S. Davidson, J. R. Ellis and K. A. Olive, Phys. Lett. B **297**, 118 (1992) [hep-ph/9302221].

[46] J. M. Cline, K. Kainulainen and K. A. Olive, Phys. Rev. D **49**, 6394 (1994) [hep-ph/9401208].